Interactions of Magnetic Pendulums

by

Razieh Sadat Saeidi Hosseini

A thesis
presented to the University of Waterloo
in fulfillment of the
thesis requirement for the degree of
Master of Applied Science
in
Systems Design Engineering

Waterloo, Ontario, Canada, 2019

I hereby declare that I am the sole author of this thesis. This is a true copy of the thesis, including any required final revisions, as accepted by my examiners.

I understand that my thesis may be made electronically available to the public.

Abstract

In recent years, coupled magnetic oscillators have received remarkable attention due to their application in vibration energy harvesting techniques and also its promising ability to help researchers to have a better understanding of atoms in a lattice behaviour. Energy harvesters scavenge ambient vibration energy and convert it into useful electrical energy. According to previous studies nonlinear mechanical attachments have received significant interest as the basis for energy harvesting systems. Another substantial field that coupled nonlinear oscillators and specifically coupled magnetic oscillators may play a crucial role in is atomic physic. Due to the qualitative similarity of the magnetic field and the electromagnetic field governing the atoms in the lattice structure in crystalline solids, investigating the coupled magnetic oscillators could help researchers to better perceive the lattice behaviour.

In this thesis, a chain of two-dimensional magnetic pendulums using an ideal point mass model as well as a rigid body model of a pendulum is investigated. The pendulums proposed in the model are to simulate the vibration of atoms in the lattice structure of crystalline solids and the attached magnets are chosen to represent the electromagnetic field governing the atoms. The nonlinear dynamics of the models through the interaction forces between the magnets has been investigated. With the aim of demonstrating the dynamics of the system completely, the equations of motion of the pendulum magnets have been analytically derived and by linearizing the equations of motion, the natural frequencies of the system have been found. The behaviour of the simulated system has been examined experimentally to assure the accuracy of the analytical approach. To achieve the intent, a simple experimental setup consisting of an array of two coupled magnetic pendulums has been introduced. Ultimately, the equations of motions of a rigid body model including the determined magnetic forces have been numerically solved and the nonlinear response of the system along with the equilibrium points and the system's frequency have been validated experimentally. The results obtained through comparing the simulated system response and the designed experiment response indicates that the simulated model can predict the behaviour of such system in reality.

Acknowledgements

I would like to thank my supervisors, Prof. Glenn Heppler and Prof. Eihab Abdel-Rahman for their unbounded guidance and encouragement throughout this research. They couldn't be more understanding and supportive.

Special thanks to my committee members Prof. Mustafa Yavuz and Prof. Nasser L. Azad for their insightful comments to improve the quality of this research.

Finally, I would like to thank my incredible husband, Mohammad, whom I couldn't have done this without his patience and unfailing support and my beloved parents who have always supported me and provided me with whatever I needed regardless of geography.

Dedication

To my best friend and husband, Mohammad, for his endless love and support and my loving parents, Mehri and Masoud, who have always been there for me and supported me in all aspects of my life.

Table of Contents

List of Tables

List of Figures

Chapter 1

Introduction and Literature Review

Coupled magnetic oscillators have received a great deal of attention due to their application in vibration energy harvesters and also their ability to help researchers better understand interactions among atoms in a lattice.

1.1 Introduction

Recent progress in automation and smart systems have necessitated the development of self- and low-powered sensors. Batteryless devices using energy harvesting techniques are an attractive alternative to battery powered devices. Energy harvesters scavenge ambient vibration energy and convert it to useful electrical energy. This energy can be stored in capacitors for later utilization or used immediately by sensors [1, 2].

Oscillators in vibration-based energy harvesting systems have generally been coupled either linearly or nonlinearly. Traditional linear harvesters have much less efficiency than the nonlinear ones. Therefore, nonlinear mechanical attachments have received significant interest as the basis for energy harvesting systems [3].

Nonlinear coupling can be categorized into two types, coupled non-magnetic oscillators and coupled magnetic oscillators, as will be detailed through different configurations in section 1.2. Coupled magnetic pendulums are one form of those coupled magnetic oscillators.

Another substantial field where coupled nonlinear oscillators, particularly coupled magnetic oscillators, may play a crucial role in is atomic physics. Due to the qualitative similarity of the magnetic field and the electromagnetic field governing the atoms in the lattice

structure in crystalline solids, the system could help researchers better understand lattice behaviour.

The goal of this research is to devise a model of two-dimensional magnetic pendulums in a chain and investigate the nonlinear dynamics of the model and the interaction forces among the pendulums. The pendulums are proposed in the model to simulate the atoms vibration in the lattice structure of the crystalline solids and the attached magnets are chosen to resemble the electromagnetic field governing the atoms. Such system may find potential application in improvement of the doping process of crystal silicon and similar materials. Ultimately, the behaviour of the system has to be examined experimentally to assure the accuracy of our analytical approach.

The following set of actions were undertaken to design and investigate the chains of magnetic pendulums. First, an idealized point mass model of a pendulum is introduced and the interaction forces between the magnets are obtained. Then, the equations of motion of the magnetic pendulums are analytically derived. Furthermore, by linearizing the equations of motion, the natural frequencies of the system are found. Finally, all the steps were carried out again for a more realistic rigid-body pendulum model.

To evaluate the validity of the model, a simple experimental setup consisting of an array of coupled magnetic pendulums was developed. To achieve this objective, a suitable pendulum and a proper suspension rod were designed.

Eventually, the equations of motion of a rigid-body model including the magnetic interaction forces were numerically solved and the nonlinear response of the system along with its equilibrium points and natural frequency were validated.

1.2 Literature Review

This section reviews various coupled oscillators that have been previously presented. It is organized as follows: in section 1.2.1 an example of linearly coupled oscillators is introduced, section 1.2.2 covers various types of nonlinearly coupled oscillators in detail, including coupled non-magnetic oscillators and coupled magnetic oscillators. A particular type of magnetically coupled oscillators, coupled magnetic pendulums, and several applications of each type are presented in section 1.2.2 as well.

1.2.1 Coupled Linear Oscillators

Linear interaction of oscillators has been considered in prior research. For instance, Belbasi et al. [4] made a linear system using linear springs to couple point masses. A forced system of N identical one-dimensional coupled oscillators, Fig. 1.1, was investigated. Dependence of the masses' displacement on the frequency of a harmonic driving force is obtained and resonance and anti-resonance frequencies are derived [4].

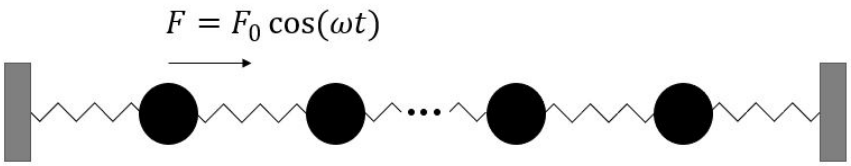

Figure 1.1: A driven system of N coupled linear oscillators.

1.2.2 Coupled Nonlinear Oscillators

In recent years, coupled nonlinear oscillators have received remarkable attention. Different forms of nonlinearly coupled oscillators has been presented. Some studies investigated non-magnetic oscillators which have been nonlinearly coupled [5, 6, 7, 8]. Other studies have focused on coupled magnetic oscillators [9, 10, 11, 12] including coupled magnetic pendulums.

Coupled Non-magnetic Oscillators

Non-magnetic masses have been coupled nonlinearly in previous studies. Jothimurugan et al. [5] investigated the frequency response of a system of N coupled Duffing oscillators where only the first oscillator is excited by an external force. Another study conducted by Gendelman et al. [6] investigated the dynamics of a linear oscillator weakly coupled to a nonlinear attachment with a small mass and studied energy pumping between them. Bitar et al. [7] analyzed the nonlinear dynamics of a weakly coupled chain of pendulums, Fig. 1.2. The system was composed of N identical planar pendulums coupled via linear torsional springs and each pendulum was subjected to an external force. A model reduction method was proposed to determine the dominant dynamics of the system. Furthermore, the basins of attraction of the system response showed that increasing the number of

coupled pendulums increase the distribution (likelihood) of the multimodal response where all pendulums collectively respond to excitation [7].

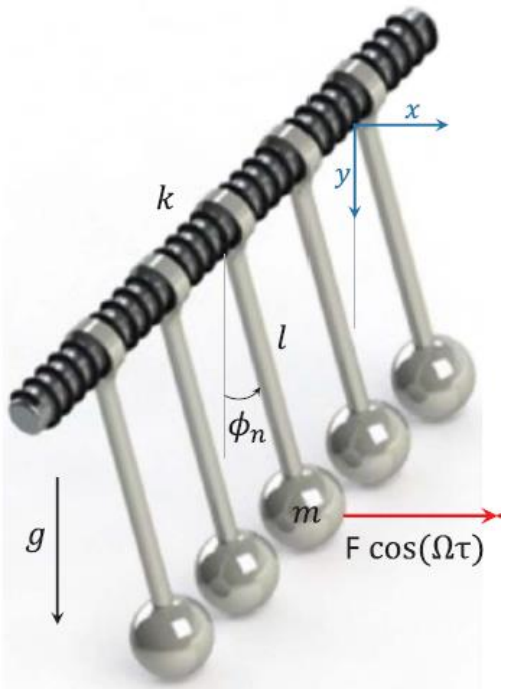

Figure 1.2: A chain of N identical pendulums [7].

In the work of Jallouli et al. [8], the dynamics of an array of coupled pendulums, Fig. 1.3, under simultaneous parametric and external excitations was investigated, with the aim of modifying the stability of the solitons in the chain. They indicated that using parametric and external excitations simultaneously enabled the transformation of a zero attractor soliton solution to a periodically stable one. Hence, the existence region of solitons can be increased by adding an external excitation [8].

Coupled Magnetic Oscillators

Magnetic interaction among magnets is a form of nonlinear coupling. Moleron et al. [9] investigated the dynamics of a one-dimensional nonlinear lattice composed of similar repelling magnets, Fig. 1.4. They obtained the system equations and found that in high-energy regime, solitary waves are localized in a single-lattice spacing [9].

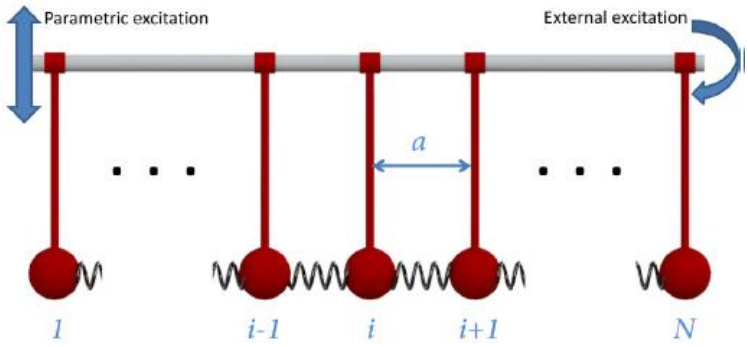

Figure 1.3: An Array of coupled non-magnetic oscillators [8].

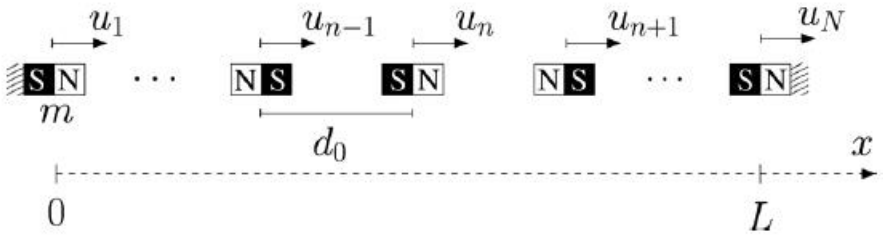

Figure 1.4: A chain of N identical magnets [9].

Magnetic interaction among magnets in other configurations has also been considered in other research. Wang et al. [10] configured a piezoelectric energy harvester as shown in Fig. 1.5. They calculated the displacement of the tip magnet on base-excited cantilever beam interacting with two external magnets using the harmonic balance and multiple-scales methods.

Different configurations of magnetic oscillators have also been investigated. Another piezoelastic energy harvester with two magneto-elastic oscillators forced by a harmonic base excitation and coupled by a load resistance, Fig. 1.6, was examined by Litak et al. [11]. In the system with relative mistuning in the stiffness of the harvesting oscillators, the dependence of the voltage output on the excitation frequency was demonstrated. There was a typical resonance curve for the total output power versus the excitation frequency, however, the harvesters worked mostly in the unsynchronized regime due to the mistuning [11].

Interactions among the magnets were observed by Tang et al. [12] as well. They proposed a magnetically coupled piezoelectric energy harvester (PEH), where a magnetic

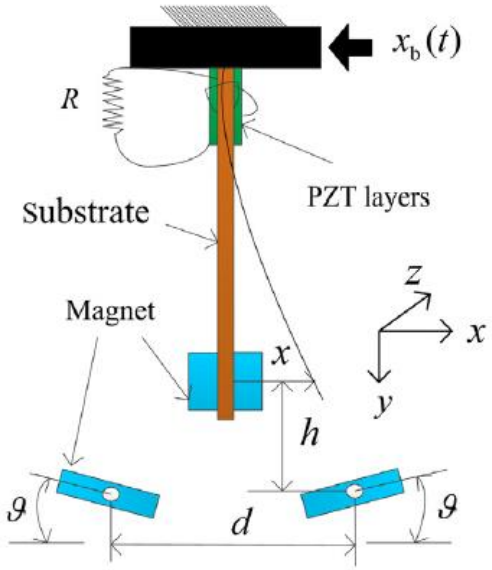

Figure 1.5: Schematic diagram of the energy harvester [10].

oscillator is used to introduce magnetic interactions. For comparison purposes, they established lumped parameter models for a conventional linear PEH, a nonlinear PEH with the fixed magnets, and a proposed PEH interacting with a magnetic oscillator, Fig. 1.7. They indicated that introducing the magnetic oscillator can broaden the operating bandwidth and simultaneously enhance the achievable power.

Coupled Magnetic Pendulums

A particular type of magnetically coupled oscillators are coupled magnetic pendulums. They consist of magnets attached to oscillating pendulums. The pendulums are, thus, coupled magnetically. One study [13] proposed a system composed of two pendulums coupled mechanically and magnetically, Fig. 1.8, to increase the magnitude and bandwidth of the output power in an electromagnetic energy harvester.

Another study presented a different configuration of a magnetic pendulum to harvest inertial energy as well as vibration energy [14]. They investigated the dynamics of the magnetic pendulum system illustrated in Fig. 1.9 to maximally harvest those energies.

Some studies have proposed using pendulum magnets as interacting particles in models of repulsive lattices. The main goal of these studies is to describe the generation and

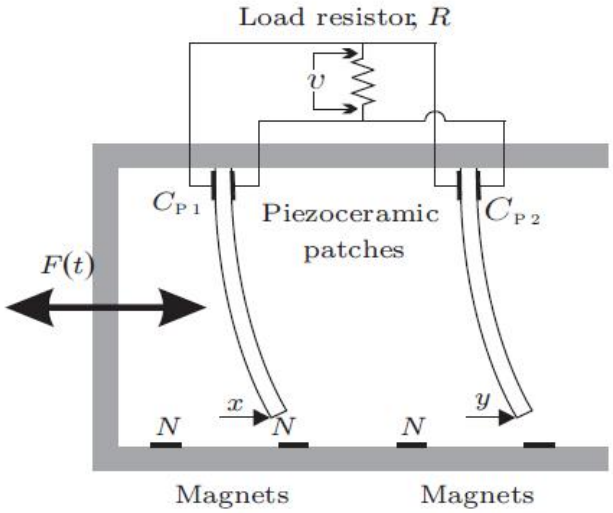

Figure 1.6: Schematic diagram of the harvester system [11].

propagation of localized perturbations. For example, Russel et al. [15] used linear and circular, Fig. 1.10, chains of magnetic pendulums. The model is composed of eighteen short dipole magnets freely suspended by rigid struts from pivots. The model assumes that the size of the magnets is small compared to the length of the struts.

More recently, Mehrem at al. [16] proposed another configuration for a chain of repelling magnets. In this case, the chain of magnets was driven dynamically by a subwoofer speaker in a similar setup to that of Russel et al. [15]. The authors studied the particular case where dipoles are in the same plane and the displacements of the magnets are assumed to be small. Magnets with small dimensions compared to their separation distance were used. Under these circumstances, the propagation of nonlinear waves in a lattice of repelling magnets was investigated. The model consists of 53 identical cylindrical magnets oriented in a one-dimensional periodic lattice as shown in Fig. 1.11.

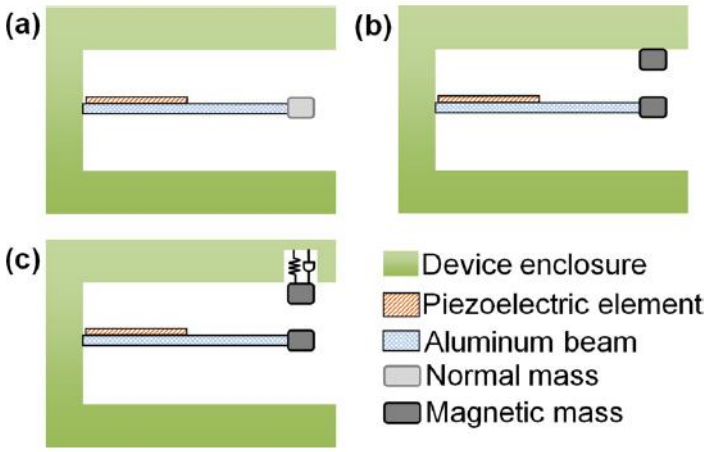

Figure 1.7: Various PEH configurations [12].

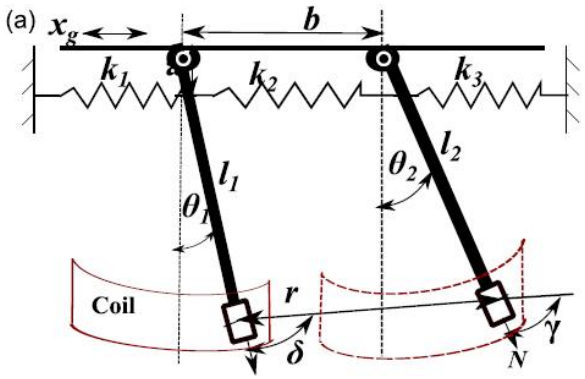

Figure 1.8: Schematic of a magneto-elastic system [13].

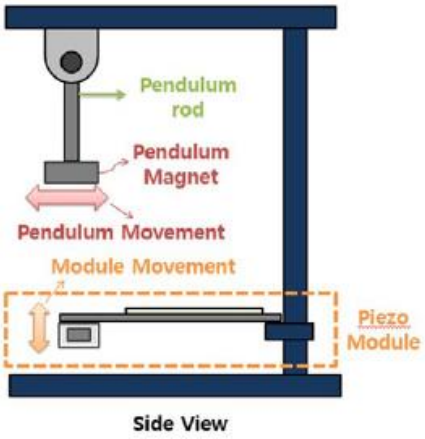

Figure 1.9: Schematic of a magnetic pendulum system [14].

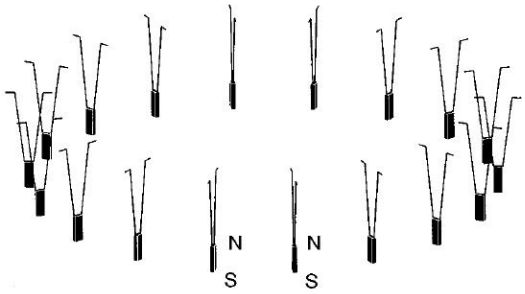

Figure 1.10: A circular chain of magnetic pendulums [15].

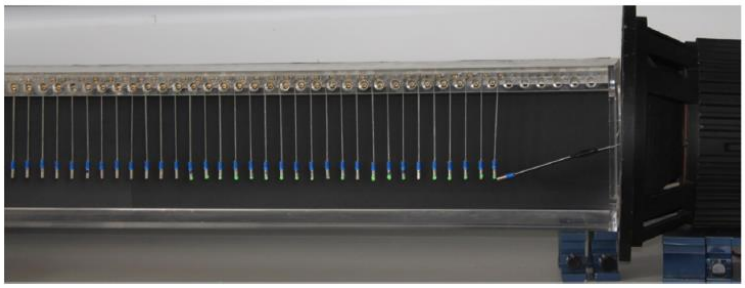

Figure 1.11: An array of pendulum magnets driven by a dynamic subwoofer speaker [16].

1.3 Thesis Layout

The thesis is organized in the following chapters: in Chapter 2 the model of magnetic pendulums is introduced and the nonlinear dynamics of the system is investigated theoretically. Chapter 3 covers the experimental design of the system of interest. In Chapter 4 the analytical response of the system is validated in comparison with the experimental results and the interaction forces pertaining to the responses are presented. Finally, conclusions and future work are discussed in Chapter 5.

Chapter 2

System Modeling

In this chapter the model of the chain of two dimensional pendulum magnets is presented and the nonlinear dynamics of the model are investigated. The interaction forces between the magnets and the equations of motion of the pendulum magnets are analytically obtained. Furthermore, by linearizing the equations of motion, the natural frequencies of the system are found.

This chapter is organized as follows: in section 2.1 ideal point mass model is introduced briefly and in section 4.5 magnetic forces are derived. Section 2.3 covers a special case of two identical point mass pendulums where the magnets are arranged so that there is a repel force between them. The rigid body model of a pendulum is investigated in section 2.5 and section 2.6 presents a special case of two identical rigid body pendulums where again they repel one another.

2.1 Ideal Point Mass Model of a Pendulum

Consider a series of N pendulums as illustrated in Fig. 2.1. Begin with establishing a fixed inertial frame with basis vectors X, Y and Z and origin O as shown. The Z basis vector is aligned with the rod that connects the pendulums, the Y basis vector is perpendicular to the ground and the X completes the right handed triad. Each pendulum is modelled as an ideal point mass pendulum of mass m_i, $i = 1, 2, \cdots N$ and length l_i. The distance between the pendulums is considered to be a. The single degree of freedom of each pendulum is the angle it makes with the vertical direction and these angles are denoted as θ_i.

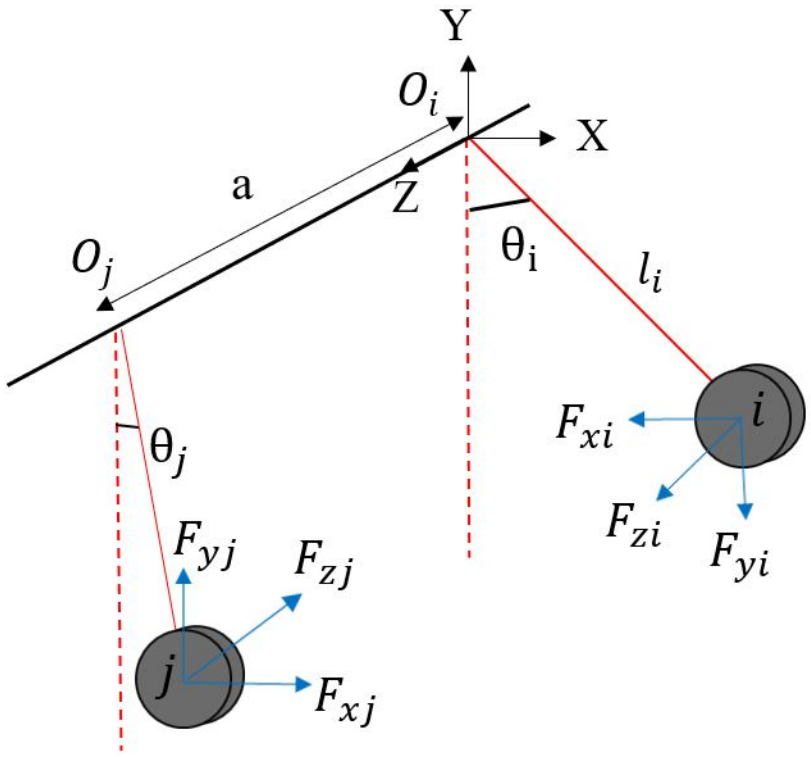

Figure 2.1: 3D view of the model.

Furthermore each pendulum mass is assumed to be magnetic and is modelled as a magnetic dipole with magnetic moment vector $\vec{\mu_i}$. If $\mu_i > 0$ then the outward normal of the magnet's north pole is directed in the same direction as Z and if $\mu_i < 0$ then the outward normal of the magnet's north pole is directed in the negative Z direction.

Figure 2.2 depicts the side view of the model when positive poles of the magnets are facing each other and there is a repulsive force between them. Hence, $\vec{\mu}_i$ and $\vec{\mu}_j$ are towards each other.

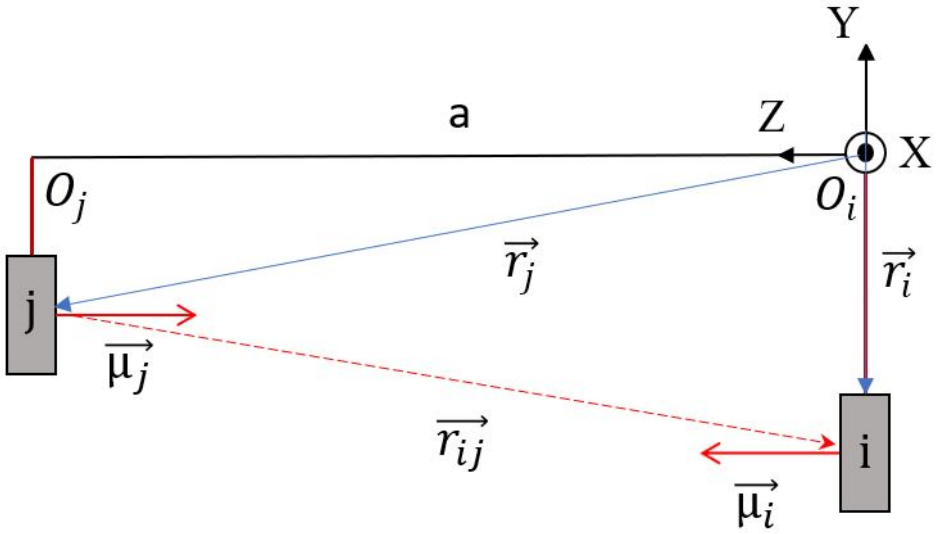

Figure 2.2: Side view of the model for repelling case.

2.2 Magnetic Forces

From Stanton et al. [17] the relation of magnetic moment vectors $\vec{\mu}_i$, the magnetic volume V_i, and the magnetization vector $\vec{M}_i$ is given by

$$\vec{\mu_i} = V_i \vec{M}_i, \quad i = 1, 2, \cdots N \tag{2.1}$$

The magnitude of the magnetization vector can be determined using

$$\vec{M}_i = \frac{\vec{B}_{ri}}{\mu_0} \quad \text{or} \quad \vec{\mu}_i = \frac{\vec{B}_{ri} V_i}{\mu_0}, \quad i = 1, 2, \cdots N \tag{2.2}$$

where magnetization vector $\vec{M}_i$ is the vector sum of all microscopic magnetic moments ($\frac{A}{m}$), $\vec{B}_{ri}$ is the magnet's residual flux density (Tesla= $\frac{Wb}{m^2}$), and μ_0 is the permeability of free space. ($\mu_0 = 4\pi \times 10^{-7}$ H/m $\simeq 12.57 \times 10^{-7}$ H/m.)

The position of a pendulum mass relative to the origin O is

$$\boldsymbol{r}_i = \begin{bmatrix} x_i \\ y_i \\ z_i \end{bmatrix} = \begin{bmatrix} l_i \sin\theta_i \\ -l_i \cos\theta_i \\ z_i \end{bmatrix}, \quad i = 1, 2, \cdots N \tag{2.3}$$

The magnetic field generated by magnet j upon magnet i is given by

$$\vec{B}_{ij} = -\frac{\mu_0}{4\pi}\vec{\nabla}\frac{\vec{\mu}_j.\vec{r}_{ij}}{\|\vec{r}_{ij}\|_2^3} \tag{2.4}$$

where $\|.\|_2$ and $\vec{\nabla}$ denote Euclidean norm and vector gradient operators and $\vec{r}_{ij}$ is the position of magnet i with respect to magnet j (or equivalently the vector from magnet j to magnet i) such that

$$\vec{r}_{ij} = \vec{r}_i - \vec{r}_j \tag{2.5}$$

or

$$\boldsymbol{r}_{ij} = \begin{bmatrix} x_{ij} \\ y_{ij} \\ z_{ij} \end{bmatrix} = \begin{bmatrix} l\sin\theta_i - l\sin\theta_j \\ -l\cos\theta_i + l\cos\theta_j \\ z_i - z_j \end{bmatrix} \tag{2.6}$$

or

$$\vec{r}_{ij} = (x_i - x_j)\hat{e}_x + (y_i - y_j)\hat{e}_y + (z_i - z_j)\hat{e}_z \tag{2.7}$$

and the magnitude of $\vec{r}_{ij}$ is

$$r_{ij} = \sqrt{(x_i - x_j)^2 + (y_i - y_j)^2 + (z_i - z_j)^2} = \sqrt{x_{ij}^2 + y_{ij}^2 + z_{ij}^2} \tag{2.8}$$

the magnetic moment vectors of magnets i and j are oriented in the z-direction.

$$\vec{\mu}_i = \mu_i\hat{e}_Z \tag{2.9a}$$
$$\vec{\mu}_j = \mu_j\hat{e}_Z \tag{2.9b}$$

The magnetic field generated by magnet j upon magnet i, $\vec{B}_{ij}$, is evaluated by using Eqs.(2.5) and (2.9b) in Eq.(2.4) as per

$$\vec{B}_{ij} = \frac{-\mu_0}{4\pi}\vec{\nabla}f \tag{2.10}$$

where

$$f = \frac{\vec{\mu}_j.\vec{r}_{ij}}{\|\vec{r}_{ij}\|_2^3} \tag{2.11}$$

$$\vec{\mu}_j.\vec{r}_{ij} = \mu_j(z_i - z_j) \tag{2.12}$$

and

$$\|\vec{r}_{ij}\|_2^3 = \left(\sqrt{(x_i - x_j)^2 + (y_i - y_j)^2 + (z_i - z_j)^2}\right)^3 \tag{2.13}$$

so that

$$f = \frac{\mu_j(z_i - z_j)}{((x_i - x_j)^2 + (y_i - y_j)^2 + (z_i - z_j)^2)^{3/2}} \tag{2.14}$$

Now

$$\vec{\nabla} f = \frac{\partial f}{\partial x}\hat{e}_x + \frac{\partial f}{\partial y}\hat{e}_y + \frac{\partial f}{\partial z}\hat{e}_z \tag{2.15}$$

$$\begin{aligned}\vec{\nabla} f =& \frac{-3\mu_j(z_j - z_i)(x_j - x_i)}{((z_j - z_i)^2 + (x_j - x_i)^2 + (y_j - y_i)^2)^{5/2}}\hat{e}_x \\ &+ \frac{-3\mu_j(z_j - z_i)(y_j - y_i)}{((z_j - z_i)^2 + (x_j - x_i)^2 + (y_j - y_i)^2)^{5/2}}\hat{e}_y \\ &+ \left(\frac{-3\mu_j(z_j - z_i)^2}{((z_j - z_i)^2 + (x_j - x_i)^2 + (y_j - y_i)^2)^{5/2}} + \frac{\mu_j}{((z_j - z_i)^2 + (x_j - x_i)^2 + (y_j - y_i)^2)^{3/2}}\right)\hat{e}_z\end{aligned} \tag{2.16}$$

Recalling equation (2.10)

$$\begin{aligned}\vec{B}_{ij} =& \frac{-\mu_0}{4\pi}\left[\frac{-3\mu_j(z_j - z_i)(x_j - x_i)}{((z_j - z_i)^2 + (x_j - x_i)^2 + (y_j - y_i)^2)^{5/2}}\hat{e}_x\right. \\ &+ \frac{-3\mu_j(z_j - z_i)(y_j - y_i)}{((z_j - z_i)^2 + (x_j - x_i)^2 + (y_j - y_i)^2)^{5/2}}\hat{e}_y \\ &\left.+ \left(\frac{-3\mu_j(z_j - z_i)^2}{((z_j - z_i)^2 + (x_j - x_i)^2 + (y_j - y_i)^2)^{5/2}} + \frac{\mu_j}{((z_j - z_i)^2 + (x_j - x_i)^2 + (y_j - y_i)^2)^{3/2}}\right)\hat{e}_z\right]\end{aligned} \tag{2.17}$$

The potential energy in the field is

$$U_m = -\vec{B}_{ij}.\vec{\mu}_i \tag{2.18}$$

which yields

$$U_m = \frac{\mu_0}{4\pi}\left(\frac{-3\mu_i\mu_j(z_j - z_i)^2}{((z_j - z_i)^2 + (x_j - x_i)^2 + (y_j - y_i)^2)^{5/2}} - \frac{-\mu_i\mu_j}{((z_j - z_i)^2 + (x_j - x_i)^2 + (y_j - y_i)^2)^{3/2}}\right) \tag{2.19}$$

The magnetic force on pendulum i due to pendulum j is determined by taking the gradient of Eq. (2.19).

$$\vec{F}_{mi} = -\vec{\nabla} U \tag{2.20}$$

where

$$\boldsymbol{F}_{mi} = \begin{bmatrix} F_{xi} \\ F_{yi} \\ F_{zi} \end{bmatrix} \tag{2.21}$$

and

$$\vec{F}_{mi} = -\left(\frac{\partial U}{\partial x}\hat{e}_x + \frac{\partial U}{\partial y}\hat{e}_y + \frac{\partial U}{\partial z}\hat{e}_z \right) \tag{2.22}$$

so that

$$\begin{aligned}
\vec{F}_{mi} = \frac{3\mu_0}{4\pi}(\mu_i\mu_j) \Bigg[& \frac{(x_i - x_j)}{((z_j - z_i)^2 + (x_j - x_i)^2 + (y_j - y_i)^2)^{5/2}} \\
& - \frac{5((z_i - z_j)^2)(x_i - x_j)}{((z_j - z_i)^2 + (x_j - x_i)^2 + (y_j - y_i)^2)^{7/2}} \Bigg] \hat{e}_x \\
+ \frac{3\mu_0}{4\pi}(\mu_i\mu_j) \Bigg[& \frac{(y_i - y_j)}{((z_j - z_i)^2 + (x_j - x_i)^2 + (y_j - y_i)^2)^{5/2}} \\
& - \frac{5((z_i - z_j)^2)(y_i - y_j)}{((z_j - z_i)^2 + (x_j - x_i)^2 + (y_j - y_i)^2)^{7/2}} \Bigg] \hat{e}_y \\
+ \frac{3\mu_0}{4\pi}(\mu_i\mu_j) \Bigg[& \frac{3(z_i - z_j)}{((z_j - z_i)^2 + (x_j - x_i)^2 + (y_j - y_i)^2)^{5/2}} \\
& - \frac{5(z_i - z_j)^3}{((z_j - z_i)^2 + (x_j - x_i)^2 + (y_j - y_i)^2)^{7/2}} \Bigg] \hat{e}_z
\end{aligned}$$

or

$$\boldsymbol{F}_{mi} = \begin{bmatrix} F_{xi} \\ F_{yi} \\ F_{zi} \end{bmatrix} = \frac{-3\mu_0\mu_i\mu_j}{4\pi} \begin{bmatrix} \frac{5x_{ij}z_{ij}^2}{r_{ij}^7} - \frac{x_{ij}}{r_{ij}^5} \\ \frac{5y_{ij}z_{ij}^2}{r_{ij}^7} - \frac{y_{ij}}{r_{ij}^5} \\ \frac{5z_{ij}^3}{r_{ij}^7} - \frac{3z_{ij}}{r_{ij}^5} \end{bmatrix} \quad i \neq j \tag{2.23}$$

In the above, if $i = j$ then it is a self force and we take $\vec{F}_{ii} = 0$. Also, it will necessarily be the case that $\vec{F}_{ji} = -\vec{F}_{ij}$. An alternate method of deriving this force is given in Appendix A.

In addition to the magnetic forces acting on pendulum i there will also be gravitational forces of the form

$$\boldsymbol{F}_{gi} = \begin{bmatrix} 0 \\ -m_i g \\ 0 \end{bmatrix} \tag{2.24}$$

Both the magnetic and the gravitational forces will generate moments about the point of suspension of each pendulum.The moment about O_i is given by

$$\vec{M}_i = \vec{r}_{Oi} \times (\vec{F}_{mi} + \vec{F}_{gi}) \tag{2.25}$$

Where the position of the magnet i is defined by the position vector $\vec{r}_{Oi}$, which extends from the point of suspension of pendulum i, O_i, to the magnet. From Fig. 2.1

$$\boldsymbol{r}_{Oi} = \begin{bmatrix} l_i \sin\theta_i \\ -l_i \cos\theta_i \\ 0 \end{bmatrix} \tag{2.26}$$

and hence from Eq. (2.25)

$$\boldsymbol{M}_i = \begin{bmatrix} l_i \sin\theta_i \\ -l_i \cos\theta_i \\ 0 \end{bmatrix} \times \begin{bmatrix} F_{xi} \\ F_{yi} - m_i g \\ F_{zi} \end{bmatrix} = \begin{bmatrix} -F_{zi}(l_i \cos\theta_i) \\ -F_{zi}(l_i \sin\theta_i) \\ (F_{yi} - m_i g)(l_i \sin\theta_i) + F_{xi}(l_i \cos\theta_i) \end{bmatrix} \tag{2.27}$$

In addition to the moments that arise due to magnetic forces and gravity there will also be reaction moments (torques) at the suspension point. These are assumed to be of the form

$$\boldsymbol{M}_{Ri} = \begin{bmatrix} T_{xi} \\ T_{yi} \\ -c_i\dot{\theta}_i \end{bmatrix} \tag{2.28}$$

where T_{xi} is the twisting moment about the X axis, T_{yi} is the bending moment about the Y axis and $-c\dot{\theta}$ is the viscous damping moment acting about the Z axis.

Euler's equation for the motion of pendulum i is

$$\vec{J}_i \,.\, \vec{\alpha}_i + \vec{\omega}_i \times \vec{J}_i \,.\, \vec{\omega}_i = \vec{M}_i + \vec{M}_{Ri} \tag{2.29}$$

where $\vec{J}_i$ is the inertia dyadic of pendulum i which is expressed in the form of

$$\boldsymbol{J}_i = \begin{bmatrix} J_{11} & 0 & 0 \\ 0 & J_{22} & 0 \\ 0 & 0 & J_{33} \end{bmatrix} \tag{2.30}$$

where $J_{11} = 0$, $J_{22} = J_{33} = m_i l_i^2$. Further, with respect to Eq. (2.29), we have that

$$\boldsymbol{\alpha}_i = \begin{bmatrix} 0 \\ 0 \\ \ddot{\theta}_i \end{bmatrix} \quad \text{and} \quad \boldsymbol{\omega}_i = \begin{bmatrix} 0 \\ 0 \\ \dot{\theta}_i \end{bmatrix} \tag{2.31}$$

where $\vec{\alpha}$ is the angular acceleration and $\vec{\omega}$ is the angular velocity.

Substituting Eq. (2.30) and Eq. (2.31) into Eq. (2.29) gives us

$$\begin{bmatrix} 0 \\ 0 \\ m_i l_i^2 \ddot{\theta}_i \end{bmatrix} = \boldsymbol{M}_i + \boldsymbol{M}_{Ri} \tag{2.32}$$

So the governing equation for pendulum i, is

$$\begin{bmatrix} 0 \\ 0 \\ m_i l_i^2 \ddot{\theta}_i \end{bmatrix} = \begin{bmatrix} -F_{zi}(l_i \cos\theta_i) \\ -F_{zi}(l_i \sin\theta_i) \\ (F_{yi} - m_i g)(l_i \sin\theta_i) + F_{xi}(l_i \cos\theta_i) \end{bmatrix} + \begin{bmatrix} T_{xi} \\ T_{yi} \\ -c_i \dot{\theta}_i \end{bmatrix} \tag{2.33}$$

From these we can see that $T_{xi} = F_{zi}(l_i \cos\theta_i)$ is twisting reaction at the suspension point and $T_{yi} = F_{zi}(l_i \sin\theta_i)$ is the time dependent bending moment at the suspension point.

2.3 Special Case: $N = 2$, Repulsion

To get a fundamental understanding of how this system behaves we will consider the special case of two identical pendulums where the magnets are arranged so that there is a repulsive force between them. We shall simplify the governing equations using the following substitutions:

$$\begin{aligned} B_{r1} &= B_{r2} = B_r \\ c_1 &= c_2 = c \\ l_1 &= l_2 = l \\ m_1 &= m_2 = m \\ M_1 &= M_2 = M \\ V_1 &= V_2 = V \\ z_1 &= 0, \qquad z_2 = \ a \\ \mu_1 &= \mu, \qquad \mu_2 = -\mu \end{aligned} \tag{2.34}$$

Note that he last two assumptions mean that the north poles of the two magnets are facing one another.

2.3.1 Pendulum 1: General Equations of Motion

The governing equations for pendulum 1 are (from Eq. (2.33))

$$\begin{bmatrix} 0 \\ 0 \\ ml^2\ddot{\theta}_1 \end{bmatrix} = \begin{bmatrix} -F_{z1}(l\cos\theta_1) \\ -F_{z1}(l\sin\theta_1) \\ (F_{y1}-mg)(l\sin\theta_1)+F_{x1}(l\cos\theta_1) \end{bmatrix} + \begin{bmatrix} T_{x1} \\ T_{y1} \\ -c\dot{\theta}_1 \end{bmatrix} \tag{2.35}$$

To find the Euler equation we will need $\vec{F}_{m1}$. Where, from Eq. (2.23), (remember that $\mu_1 = \mu$ and $\mu_2 = -\mu$)

$$\boldsymbol{F}_{m1} = \begin{bmatrix} F_{x1} \\ F_{y1} \\ F_{z1} \end{bmatrix} = \frac{3\mu_0\mu^2}{4\pi} \begin{bmatrix} \frac{5x_{12}z_{12}^2}{r_{12}^7} - \frac{x_{12}}{r_{12}^5} \\ \frac{5y_{12}z_{12}^2}{r_{12}^7} - \frac{y_{12}}{r_{12}^5} \\ \frac{5z_{12}^3}{r_{12}^7} - \frac{3z_{12}}{r_{12}^5} \end{bmatrix} \tag{2.36}$$

Recall from Eq. (2.6)

$$\boldsymbol{r}_{12} = \begin{bmatrix} x_{12} \\ y_{12} \\ z_{12} \end{bmatrix} = \begin{bmatrix} l\sin\theta_1 - l\sin\theta_2 \\ -l\cos\theta_1 + l\cos\theta_2 \\ -a \end{bmatrix} \tag{2.37}$$

and from Eq. (2.8)

$$r_{12} = \sqrt{(l\sin\theta_1 - l\sin\theta_2)^2 + (-l\cos\theta_1 + l\cos\theta_2)^2 + a^2} = \sqrt{a^2 + 2l^2(1-\cos(\theta_2-\theta_1))} \tag{2.38}$$

Also, from Eq. (2.24)

$$\boldsymbol{F}_{g1} = \begin{bmatrix} 0 \\ -mg \\ 0 \end{bmatrix} \tag{2.39}$$

so the total force acting on pendulum 1 is

$$\boldsymbol{F}_{m1} + \boldsymbol{F}_{g1} = \begin{bmatrix} \frac{3\mu_0\mu^2}{4\pi}\left(\frac{5x_{12}z_{12}^2}{r_{12}^7} - \frac{x_{12}}{r_{12}^5}\right) \\ \frac{3\mu_0\mu^2}{4\pi}\left(\frac{5y_{12}z_{12}^2}{r_{12}^7} - \frac{y_{12}}{r_{12}^5}\right) - mg \\ \frac{3\mu_0\mu^2}{4\pi}\left(\frac{5z_{12}^3}{r_{12}^7} - \frac{3z_{12}}{r_{12}^5}\right) \end{bmatrix} \tag{2.40}$$

and therefore Euler's equation for θ_1 (from Eq. (2.35)) is

$$ml^2\ddot{\theta}_1 = (F_{y1}-mg)(l\sin\theta_1) + F_{x1}(l\cos\theta_1) - c\dot{\theta}_1 \tag{2.41}$$

which is the complete nonlinear equation of motion for pendulum 1. Divide through by ml^2 to find

$$\ddot{\theta}_1 + \left(\frac{c}{ml^2}\right)\dot{\theta}_1 - \left(\frac{F_{y1}}{ml} - \frac{g}{l}\right)\sin\theta_1 - \left(\frac{F_{x1}}{ml}\right)\cos\theta_1 = 0 \tag{2.42}$$

2.3.2 Pendulum 2: General Equations of Motion

The governing equations for pendulum 2 are (from Eq. (2.33))

$$\begin{bmatrix} 0 \\ 0 \\ ml^2\ddot{\theta}_2 \end{bmatrix} = \begin{bmatrix} -F_{z2}(l\cos\theta_2) \\ -F_{z2}(l\sin\theta_2) \\ (F_{y2} - mg)(l\sin\theta_1) + F_{x2}(l\cos\theta_2) \end{bmatrix} + \begin{bmatrix} T_{x2} \\ T_{y2} \\ -c\dot{\theta}_2 \end{bmatrix} \tag{2.43}$$

To find the Euler equation we will need $\vec{F}_{m2}$. Where, from Eq. (2.23), (again $\mu_1 = \mu$ and $\mu_2 = -\mu$)

$$\boldsymbol{F}_{m2} = \begin{bmatrix} F_{x2} \\ F_{y2} \\ F_{z2} \end{bmatrix} = \frac{3\mu_0\mu^2}{4\pi}\begin{bmatrix} \frac{5x_{21}z_{21}^2}{r_{21}^7} - \frac{x_{21}}{r_{21}^5} \\ \frac{5y_{21}z_{21}^2}{r_{21}^7} - \frac{y_{21}}{r_{21}^5} \\ \frac{5z_{21}^3}{r_{21}^7} - \frac{3z_{21}}{r_{21}^5} \end{bmatrix} \tag{2.44}$$

It should be noted that $r_{21} = r_{12}$ which can be demonstrated as follows.

$$\boldsymbol{r}_{21} = \begin{bmatrix} x_{21} \\ y_{21} \\ z_{21} \end{bmatrix} = \begin{bmatrix} l\sin\theta_2 - l\sin\theta_1 \\ -l\cos\theta_2 + l\cos\theta_1 \\ a \end{bmatrix} \tag{2.45}$$

So from Eq. (2.8)

$$r_{21} = \sqrt{(l\sin\theta_2 - l\sin\theta_1)^2 + (-l\cos\theta_2 + l\cos\theta_1)^2 + a^2} = \sqrt{a^2 + 2l^2(1 - \cos(\theta_2 - \theta_1))} \tag{2.46}$$

The gravity force vector $\vec{F}_{g2} = \vec{F}_{g1}$ as given in Eq. (2.39) so the total force acting on pendulum 2 is

$$\boldsymbol{F}_{m2} + \boldsymbol{F}_{g2} = \begin{bmatrix} \frac{3\mu_0\mu^2}{4\pi}\left(\frac{5x_{21}z_{21}^2}{r_{21}^7} - \frac{x_{21}}{r_{21}^5}\right) \\ \frac{3\mu_0\mu^2}{4\pi}\left(\frac{5y_{21}z_{21}^2}{r_{21}^7} - \frac{y_{21}}{r_{21}^5}\right) - mg \\ \frac{3\mu_0\mu^2}{4\pi}\left(\frac{5z_{21}^3}{r_{21}^7} - \frac{3z_{21}}{r_{21}^5}\right) \end{bmatrix} \tag{2.47}$$

and therefore Euler's equation for θ_1 (from Eq. (2.43)) is

$$ml^2\ddot{\theta}_2 = (F_{y2} - mg)(l\sin\theta_2) + F_{x2}(l\cos\theta_2) - c\dot{\theta}_2 \tag{2.48}$$

which is the complete nonlinear equation of motion for pendulum 2. Divide through by ml^2 to find

$$\ddot{\theta}_2 + \left(\frac{c}{ml^2}\right)\dot{\theta}_2 - \left(\frac{F_{y2}}{ml} - \frac{g}{l}\right)\sin\theta_2 - \left(\frac{F_{x2}}{ml}\right)\cos\theta_2 = 0 \tag{2.49}$$

2.4 Linearization

Again we will consider the special case of two identical pendulums where the magnets are arranged so that there is a repulsive force between them.

2.4.1 Pendulum 1: Force Linearization

The forces acting on pendulum 1, when the magnets are arranged in repulsion, are of the form (see Eq. (2.36))

$$\begin{aligned} F_{x1} =& \frac{-3\mu_0\,\mu^2}{4\pi}\hat{F}_{x1} \\ F_{y1} =& \frac{-3\mu_0\,\mu^2}{4\pi}\hat{F}_{y1} \\ F_{z1} =& \frac{-3\mu_0\,\mu^2}{4\pi}\hat{F}_{z1} \end{aligned} \tag{2.50}$$

with

$$\begin{aligned} \hat{F}_{x1} =& \frac{x_{12}}{r_{12}^5} - 5\,\frac{x_{12}\,{z_{12}}^2}{r_{12}^7} \\ \hat{F}_{y1} =& \frac{y_{12}}{r_{12}^5} - 5\,\frac{y_{12}\,{z_{12}}^2}{r_{12}^7} \\ \hat{F}_{z1} =& 3\,\frac{z_{12}}{r_{12}^5} - 5\,\frac{{z_{12}}^3}{r_{12}^7} \end{aligned} \tag{2.51}$$

where the position of pendulum 1 with respect to pendulum 2 is

$$\begin{aligned} x_{12} =& l\,\left(\sin\theta_1 - \sin\theta_2\right) \\ y_{12} =& l\,\left(-\cos\theta_1 + \cos\theta_2\right) \\ z_{12} =& -a \end{aligned} \tag{2.52}$$

and

$$\begin{aligned} r_{12} =& \sqrt{2\,l^2(1-\cos(\theta_1-\theta_2))+a^2} \\ =& \sqrt{2\,l^2(1-\cos(\theta_2-\theta_1))+a^2} \end{aligned} \tag{2.53}$$

Linearize about an equilibrium point which will be at a general configuration denoted by θ_{1_0} and θ_{2_0}. Therefore we assume

$$\theta_1 = \theta_{1_0} + \hat{\theta}_1, \quad \text{and} \quad \theta_2 = \theta_{2_0} + \hat{\theta}_2 \tag{2.54}$$

which upon substitution into the previous forms of $\hat{F}_{i1}$ yields

$$\begin{aligned} \hat{F}_{x1} =& \frac{l\,(\sin\theta_1 - \sin\theta_2)}{r_{12}^5} - 5\,\frac{l\,(\sin\theta_1 - \sin\theta_2)\,a^2}{r_{12}^7} \\ \hat{F}_{y1} =& \frac{l\,(\cos\theta_2 - \cos\theta_1)}{r_{12}^5} - 5\,\frac{l\,(\cos\theta_2 - \cos\theta_1)\,a^2}{r_{12}^7} \\ \hat{F}_{z1} =& -3\,\frac{a}{r_{12}^5} + 5\,\frac{a^3}{r_{12}^7} \end{aligned} \tag{2.55}$$

Linearizing about θ_{1_0} and θ_{2_0} for $\hat{\theta}_1 \ll 1$ and $\hat{\theta}_2 \ll 1$ we get

$$\begin{aligned} \hat{F}_{x1} =& \hat{F}_{11_0} + \hat{F}_{11_1}\,\hat{\theta}_1 + \hat{F}_{11_2}\,\hat{\theta}_2 \\ \hat{F}_{x1} =& -2\,\frac{l\,(l^2\,(1-\cos(\theta_{1_0}-\theta_{2_0}))-2\,a^2)\,(\sin\theta_{2_0}-\sin\theta_{1_0})}{r_0^7} \\ &+\left[10\,\frac{l^3\,(l^2\,(1-\cos(\theta_{1_0}-\theta_{2_0}))-3\,a^2)\,(\sin\theta_{2_0}-\sin\theta_{1_0})\sin\left(\theta_{1_0}-\theta_{2_0}\right)}{r_0^9}\right. \\ &\qquad\left.+2\,\frac{l\,(l^2\,(1-\cos(\theta_{1_0}-\theta_{2_0}))-2\,a^2)\cos\theta_{1_0}}{r_0^7}\right]\hat{\theta}_1 \\ &-\left[10\,\frac{l^3\,(l^2\,(1-\cos(\theta_{1_0}-\theta_{2_0}))-3\,a^2)\,(\sin\theta_{2_0}-\sin\theta_{1_0})\sin\left(\theta_{1_0}-\theta_{2_0}\right)}{r_0^9}\right. \\ &\qquad\left.+2\,\frac{l\,(l^2\,(1-\cos(\theta_{1_0}-\theta_{2_0}))-2\,a^2)\cos\theta_{2_0}}{r_0^7}\right]\hat{\theta}_2 \end{aligned} \tag{2.56}$$

$$
\begin{aligned}
\hat{F}_{y1} =& \hat{F}_{21_0} + \hat{F}_{21_1}\,\hat{\theta}_1 + \hat{F}_{21_2}\,\hat{\theta}_2 \\
\hat{F}_{y1} =& 2\,\frac{l\,\left(l^2\,(1-\cos(\theta_{1_0}-\theta_{2_0}))-2\,a^2\right)(\cos\theta_{2_0}-\cos\theta_{1_0})}{r_0^7} \\
&-\left[10\,\frac{l^3\,\left(l^2\,(1-\cos(\theta_{1_0}-\theta_{2_0}))-3\,a^2\right)(\cos\theta_{2_0}-\cos\theta_{1_0})\sin\left(\theta_{1_0}-\theta_{2_0}\right)}{r_0^9}\right. \\
&\qquad\left.-2\,\frac{l\,\left(l^2\,(1-\cos(\theta_{1_0}-\theta_{2_0}))-2\,a^2\right)\sin\theta_{1_0}}{r_0^7}\right]\hat{\theta}_1 \\
&+\left[10\,\frac{l^3\,\left(l^2\,(1-\cos(\theta_{1_0}-\theta_{2_0}))-3\,a^2\right)(\cos\theta_{2_0}-\cos\theta_{1_0})\sin\left(\theta_{1_0}-\theta_{2_0}\right)}{r_0^9}\right. \\
&\qquad\left.-2\,\frac{l\,\left(l^2\,(1-\cos(\theta_{1_0}-\theta_{2_0}))-2\,a^2\right)\sin\theta_{2_0}}{r_0^7}\right]\hat{\theta}_2
\end{aligned}
\tag{2.57}
$$

$$
\begin{aligned}
\hat{F}_{z1} =& \hat{F}_{31_0} + \hat{F}_{31_1}\,\hat{\theta}_1 + \hat{F}_{31_2}\,\hat{\theta}_2 \\
\hat{F}_{z1} =& -2\,\frac{a\,\left(3\,l^2\,(1-\cos(\theta_{1_0}-\theta_{2_0}))-a^2\right)}{r_0^7} \\
&-\left[\left(30\,\frac{a\,l^4\,\cos\left(\theta_{1_0}-\theta_{2_0}\right)}{r_0^9}-5\,\frac{a\,l^2\,\left(6\,l^2-4\,a^2\right)}{r_0^9}\right)\sin\left(\theta_{1_0}-\theta_{2_0}\right)\right]\hat{\theta}_1 \\
&+\left[\left(30\,\frac{a\,l^4\,\cos\left(\theta_{1_0}-\theta_{2_0}\right)}{r_0^9}-5\,\frac{a\,l^2\,\left(6\,l^2-4\,a^2\right)}{r_0^9}\right)\sin\left(\theta_{1_0}-\theta_{2_0}\right)\right]\hat{\theta}_2
\end{aligned}
\tag{2.58}
$$

where

$$
r_0 = \sqrt{2\,l^2(1-\cos(\theta_{1_0}-\theta_{2_0}))+a^2} = \sqrt{2\,l^2(1-\cos(\theta_{2_0}-\theta_{1_0}))+a^2} \tag{2.59}
$$

Note that

$$
r_0 = r_{12}\big|_{\substack{\hat{\theta}_1=0,\\ \hat{\theta}_2=0}} \tag{2.60}
$$

2.4.2 Pendulum 1: Linearized Equations of Motion

The equation of motion for pendulum 1 is therefore (see Eq. 2.41), for $\hat{\theta}_1 \ll 1$ and $\hat{\theta}_2 \ll 1$,

$$\begin{aligned}
ml^2\ddot{\theta}_1 + c\dot{\theta}_1 =& l\left((F_{y1} - mg)\sin\theta_1 + F_{x1}\cos\theta_1\right) \\
ml^2\ddot{\theta}_1 + c\dot{\theta}_1 =& \frac{-3l\,\mu_0\,\mu^2}{4\pi}(\hat{F}_{y1}\sin\theta_1 + \hat{F}_{x1}\cos\theta_1) - mgl\sin\theta_1 \\
ml^2(\ddot{\theta}_{1_0} + \ddot{\hat{\theta}}_1) + c(\dot{\theta}_{1_0} + \dot{\hat{\theta}}_1) =& \frac{-3l\,\mu_0\,\mu^2}{4\pi}(\hat{F}_{y1}\sin(\theta_{1_0} + \hat{\theta}_1) - \hat{F}_{x1}\cos(\theta_{1_0} + \hat{\theta}_1)) \\
& - mgl\sin(\theta_{1_0} + \hat{\theta}_1) \\
ml^2\ddot{\hat{\theta}}_1 + c\dot{\hat{\theta}}_1 =& \frac{-3l\,\mu_0\,\mu^2}{4\pi}\Big(\hat{F}_{y1}(\sin\theta_{1_0}\cos\hat{\theta}_1 + \cos\theta_{1_0}\sin\hat{\theta}_1) \\
& \qquad -\hat{F}_{x1}(\cos\theta_{1_0}\cos\hat{\theta}_1 - \sin\theta_{1_0}\sin\hat{\theta}_1)\Big) \\
& - mgl\,(\sin\theta_{1_0}\cos\hat{\theta}_1 + \cos\theta_{1_0}\sin\hat{\theta}_1)
\end{aligned} \tag{2.61}$$

Recalling that $\hat{\theta}_1 \ll 1$ this can be written as

$$\begin{aligned}
ml^2\ddot{\hat{\theta}}_1 + c\dot{\hat{\theta}}_1 =& \frac{-3l\,\mu_0\,\mu^2}{4\pi}\left(\hat{F}_{y1}(\sin\theta_{1_0} + \cos\theta_{1_0}\hat{\theta}_1) - \hat{F}_{x1}(\cos\theta_{1_0} - \sin\theta_{1_0}\hat{\theta}_1)\right) \\
& - mgl\,(\sin\theta_{1_0} + \cos\theta_{1_0}\hat{\theta}_1) \\
ml^2\ddot{\hat{\theta}}_1 + c\dot{\hat{\theta}}_1 =& \frac{-3l\,\mu_0\,\mu^2}{4\pi}\left(\hat{F}_{y1}\sin\theta_{1_0} + \hat{F}_{y1}\cos\theta_{1_0}\hat{\theta}_1 - \hat{F}_{x1}\cos\theta_{1_0} + \hat{F}_{x1}\sin\theta_{1_0}\hat{\theta}_1\right) \\
& - mg\,l\sin\theta_{1_0} - mg\,l\cos\theta_{1_0}\hat{\theta}_1
\end{aligned} \tag{2.62}$$

Linearizing the products $F_{x1}l\hat{\theta}_1$ and $F_{y1}l\hat{\theta}_1$ yields

$$\begin{aligned}
F_{x1}\,l\,\hat{\theta}_1 = F_{11_0}\,l\,\hat{\theta}_1 &= \left(\frac{-3\mu_0\,\mu^2}{4\pi}\right)\left[-2\,\frac{l\,(l^2\,(1-\cos(\theta_{1_0}-\theta_{2_0})) - 2\,a^2)\,(\sin\theta_{2_0} - \sin\theta_{1_0})}{r_0^7}\right]\hat{\theta}_1 \\
F_{y1}\,l\,\hat{\theta}_1 = F_{21_0}\,l\,\hat{\theta}_1 &= \left(\frac{-3\mu_0\,\mu^2}{4\pi}\right)\left[2\,\frac{l\,(l^2\,(1-\cos(\theta_{1_0}-\theta_{2_0})) - 2\,a^2)\,(\cos\theta_{2_0} - \cos\theta_{1_0})}{r_0^7}\right]\hat{\theta}_1
\end{aligned} \tag{2.63}$$

Upon substituting the derived linearized expressions for F_{x1} and F_{y1} into the right hand

side of the equation of motion we obtain

$$
\begin{aligned}
m l^2 \ddot{\hat{\theta}}_1 + c \dot{\hat{\theta}}_1 = & - m g\, l\, \cos\theta_{1_0}\, \hat{\theta}_1 \\
& - \left(\frac{-3\mu_0\, \mu^2}{4\pi} \right) \left[10\, \frac{l^4\, \left(l^2 \left(1 - \cos(\theta_{1_0} - \theta_{2_0}) \right) - 3\, a^2 \right) \sin^2 \left(\theta_{1_0} - \theta_{2_0} \right)}{r_0^9} \right. \\
& \qquad \left. -2\, \frac{l^2\, \left(l^2 \left(1 - \cos(\theta_{1_0} - \theta_{2_0}) \right) - 2\, a^2 \right) \cos(\theta_{1_0} - \theta_{2_0})}{r_0^7} \right] \hat{\theta}_1 \\
& + \left(\frac{-3\mu_0\, \mu^2}{4\pi} \right) \left[10\, \frac{l^4\, \left(l^2 \left(1 - \cos(\theta_{1_0} - \theta_{2_0}) \right) - 3\, a^2 \right) \sin^2 \left(\theta_{1_0} - \theta_{2_0} \right)}{r_0^9} \right. \\
& \qquad \left. -2\, \frac{l^2\, \left(l^2 \left(1 - \cos(\theta_{1_0} - \theta_{2_0}) \right) - 2\, a^2 \right) \cos(\theta_{1_0} - \theta_{2_0})}{r_0^7} \right] \hat{\theta}_2 \\
& - \left(\frac{-3\mu_0\, \mu^2}{4\pi} \right) \left[2\, \frac{l^2\, \left(l^2 \left(1 - \cos(\theta_{1_0} - \theta_{2_0}) \right) - 2\, a^2 \right) \left(\cos\theta_{1_0} - \cos\theta_{2_0} \right) \sin\theta_{1_0}}{r_0^7} \right. \\
& \qquad \left. -2\, \frac{l^2\, \left(l^2 \left(1 - \cos(\theta_{1_0} - \theta_{2_0}) \right) - 2\, a^2 \right) \left(\sin\theta_{1_0} - \sin\theta_{2_0} \right) \cos\theta_{1_0}}{r_0^7} \right] \\
& - m g\, l\, \sin\theta_{1_0}
\end{aligned}
\tag{2.64}
$$

2.4.3 Pendulum 2: Force Linearization

The forces acting on pendulum 2 are of the form (see Eq. (2.44))

$$
\begin{aligned}
F_{x2} = & \frac{-3\mu_0\, \mu^2}{4\pi} \hat{F}_{x2} \\
F_{y2} = & \frac{-3\mu_0\, \mu^2}{4\pi} \hat{F}_{y2} \\
F_{z2} = & \frac{-3\mu_0\, \mu^2}{4\pi} \hat{F}_{z2}
\end{aligned}
\tag{2.65}
$$

with

$$
\begin{aligned}
\hat{F}_{x2} = & \frac{x_{21}}{r_{21}^5} - 5\, \frac{x_{21}\, {z_{21}}^2}{r_{21}^7} \\
\hat{F}_{y2} = & \frac{y_{21}}{r_{21}^5} - 5\, \frac{y_{21}\, {z_{21}}^2}{r_{21}^7} \\
\hat{F}_{z2} = & 3\, \frac{z_{21}}{r_{21}^5} - 5\, \frac{{z_{21}}^3}{r_{21}^7}
\end{aligned}
\tag{2.66}
$$

where the position of pendulum 1 with respect to pendulum 2 is

$$\begin{aligned} x_{21} =& l\ (\sin\theta_2 - \sin\theta_1) \\ y_{21} =& l\ (-\cos\theta_2 + \cos\theta_1) \\ z_{21} =& a \end{aligned} \tag{2.67}$$

and

$$\begin{aligned} r_{21} =& \sqrt{2\,l^2(1-\cos(\theta_2-\theta_1))+a^2} \\ =& \sqrt{2\,l^2(1-\cos(\theta_1-\theta_2))+a^2} \\ =& r_{12} \end{aligned} \tag{2.68}$$

Linearize about an equilibrium point which will be at a general configuration denoted by θ_{1_0} and θ_{2_0}. Therefore we again assume

$$\theta_1 = \theta_{1_0} + \hat{\theta}_1, \quad \text{and} \quad \theta_2 = \theta_{2_0} + \hat{\theta}_2 \tag{2.69}$$

which upon substitution into the previous forms of $\hat{F}_{i2}$ yields

$$\begin{aligned} \hat{F}_{x2} =& \frac{l\ (\sin\theta_2 - \sin\theta_1)}{r_0^5} - 5\,\frac{l\ (\sin\theta_2 - \sin\theta_1)\,a^2}{r_0^7} \\ \hat{F}_{y2} =& \frac{l\ (-\cos\theta_2 + \cos\theta_1)}{r_0^5} - 5\,\frac{l\ (-\cos\theta_2 + \cos\theta_1)\,a^2}{r_0^7} \\ \hat{F}_{z2} =& 3\,\frac{a}{r_0^5} - 5\,\frac{a^3}{r_0^7} \end{aligned} \tag{2.70}$$

Linearizing about θ_{1_0} and θ_{2_0} for $\hat{\theta}_1 \ll 1$ and $\hat{\theta}_2 \ll 1$ we get

$$\begin{aligned} \hat{F}_{x2} =& \hat{F}_{12_0} + \hat{F}_{12_1}\,\hat{\theta}_1 + \hat{F}_{12_2}\,\hat{\theta}_2 \\ \hat{F}_{x2} =& 2\,\frac{l\ (l^2\,(1-\cos(\theta_{1_0}-\theta_{2_0}))-2\,a^2)\,(\sin\theta_{2_0}-\sin\theta_{1_0})}{r_0^7} \\ & - \left[10\,\frac{l^3\,(l^2\,(1-\cos(\theta_{1_0}-\theta_{2_0}))-3\,a^2)\,(\sin\theta_{2_0}-\sin\theta_{1_0})\sin(\theta_{1_0}-\theta_{2_0})}{r_0^9}\right. \\ & \left. +2\,\frac{l\ (l^2\,(1-\cos(\theta_{1_0}-\theta_{2_0}))-2\,a^2)\cos\theta_{1_0}}{r_0^7}\right]\hat{\theta}_1 \\ & + \left[10\,\frac{l^3\,(l^2\,(1-\cos(\theta_{1_0}-\theta_{2_0}))-3\,a^2)\,(\sin\theta_{2_0}-\sin\theta_{1_0})\sin(\theta_{1_0}-\theta_{2_0})}{r_0^9}\right. \\ & \left. +2\,\frac{l\ (l^2\,(1-\cos(\theta_{1_0}-\theta_{2_0}))-2\,a^2)\cos\theta_{2_0}}{r_0^7}\right]\hat{\theta}_2 \end{aligned} \tag{2.71}$$

$$
\begin{aligned}
\hat{F}_{y2} =& \hat{F}_{22_0} + \hat{F}_{22_1}\,\hat{\theta}_1 + \hat{F}_{22_2}\,\hat{\theta}_2 \\
\hat{F}_{y2} =& -2\,\frac{l\,\left(l^2\,(1-\cos(\theta_{1_0}-\theta_{2_0}))-2\,a^2\right)(\cos\theta_{2_0}-\cos\theta_{1_0})}{r_0^7} \\
&+\left[10\,\frac{l^3\,\left(l^2\,(1-\cos(\theta_{1_0}-\theta_{2_0}))-3\,a^2\right)(\cos\theta_{2_0}-\cos\theta_{1_0})\sin\left(\theta_{1_0}-\theta_{2_0}\right)}{r_0^9}\right. \\
&\quad\left.-2\,\frac{l\,\left(l^2\,(1-\cos(\theta_{1_0}-\theta_{2_0}))-2\,a^2\right)\sin\theta_{1_0}}{r_0^7}\right]\hat{\theta}_1 \\
&-\left[10\,\frac{l^3\,\left(l^2\,(1-\cos(\theta_{1_0}-\theta_{2_0}))-3\,a^2\right)(\cos\theta_{2_0}-\cos\theta_{1_0})\sin\left(\theta_{1_0}-\theta_{2_0}\right)}{r_0^9}\right. \\
&\quad\left.-2\,\frac{l\,\left(l^2\,(1-\cos(\theta_{1_0}-\theta_{2_0}))-2\,a^2\right)\sin\theta_{2_0}}{r_0^7}\right]\hat{\theta}_2
\end{aligned}
\tag{2.72}
$$

$$
\begin{aligned}
\hat{F}_{z2} =& \hat{F}_{32_0} + \hat{F}_{32_1}\,\hat{\theta}_1 + \hat{F}_{32_2}\,\hat{\theta}_2 \\
\hat{F}_{z2} =& 2\,\frac{a\,\left(3\,l^2\,(1-\cos(\theta_{1_0}-\theta_{2_0}))-a^2\right)}{r_0^7} \\
&+\left[\left(30\,\frac{a\,l^4\,\cos\left(\theta_{1_0}-\theta_{2_0}\right)}{r_0^9}-5\,\frac{a\,l^2\,\left(6\,l^2-4\,a^2\right)}{r_0^9}\right)\sin\left(\theta_{1_0}-\theta_{2_0}\right)\right]\hat{\theta}_1 \\
&-\left[\left(30\,\frac{a\,l^4\,\cos\left(\theta_{1_0}-\theta_{2_0}\right)}{r_0^9}-5\,\frac{a\,l^2\,\left(6\,l^2-4\,a^2\right)}{r_0^9}\right)\sin\left(\theta_{1_0}-\theta_{2_0}\right)\right]\hat{\theta}_2
\end{aligned}
\tag{2.73}
$$

Observe that $\hat{F}_{x2} = -\hat{F}_{x1}$, $\hat{F}_{y2} = -\hat{F}_{y1}$ and $\hat{F}_{z2} = -\hat{F}_{z1}$ as expected.

2.4.4 Pendulum 2: Linearized Equations of Motion

The equation of motion for pendulum 2 is therefore (see Eq. (2.48)), for $\hat{\theta}_1 \ll 1$ and $\hat{\theta}_2 \ll 1$,

$$\begin{aligned}
m l^2 \ddot{\theta}_2 + c\dot{\theta}_2 =& l\left((F_{y2} \; - mg)\sin\theta_2 + F_{x2}\,\cos\theta_2\right) \\
m l^2 \ddot{\theta}_2 + c\dot{\theta}_2 =& \frac{-3l\,\mu_0\,\mu^2}{4\pi}(\hat{F}_{y2}\,\sin\theta_2 + \hat{F}_{x2}\,\cos\theta_2) - mg\,l\,\sin\theta_2 \\
m l^2(\ddot{\theta}_{2_0} + \ddot{\hat{\theta}}_2) + c(\dot{\theta}_{2_0} + \dot{\hat{\theta}}_2) =& \frac{-3l\,\mu_0\,\mu^2}{4\pi}(\hat{F}_{y2}\,\sin(\theta_{2_0} + \hat{\theta}_2) + \hat{F}_{x2}\,\cos(\theta_{2_0} + \hat{\theta}_2)) - mg\,l\,\sin(\theta_{2_0} + \hat{\theta}_2) \\
m l^2 \ddot{\hat{\theta}}_2 + c\dot{\hat{\theta}}_2 =& \frac{-3l\,\mu_0\,\mu^2}{4\pi}\Big(\hat{F}_{y2}\,(\sin\theta_{2_0}\cos\hat{\theta}_2 + \cos\theta_{2_0}\sin\hat{\theta}_2) \\
& \qquad + \hat{F}_{x2}\,(\cos\theta_{2_0}\cos\hat{\theta}_2 - \sin\theta_{2_0}\sin\hat{\theta}_2)\Big) \\
& - mg\,l\,(\sin\theta_{2_0}\cos\hat{\theta}_2 + \cos\theta_{2_0}\sin\hat{\theta}_2) \\
m l^2 \ddot{\hat{\theta}}_2 + c\dot{\hat{\theta}}_2 =& \frac{-3l\,\mu_0\,\mu^2}{4\pi}\Big(\hat{F}_{y2}\,(\sin\theta_{2_0} + \cos\theta_{2_0}\hat{\theta}_2) + \hat{F}_{x2}\,(\cos\theta_{2_0} - \sin\theta_{2_0}\,\hat{\theta}_2)\Big) \\
& - mg\,l\,(\sin\theta_{2_0} + \cos\theta_{2_0}\,\hat{\theta}_2)
\end{aligned} \tag{2.74}$$

Linearizing the products $F_{x2}\,l\,\hat{\theta}_2$ and $F_{y2}\,l\,\hat{\theta}_2$ yields

$$\begin{aligned}
F_{x2}\,l\,\hat{\theta}_2 = F_{12_0}\,l\,\hat{\theta}_2 &= \left(\frac{-3\mu_0\,\mu^2}{4\pi}\right)\left[2\,\frac{l\;(l^2\,(1-\cos(\theta_{1_0}-\theta_{2_0}))-2\,a^2)\,(\sin\theta_{2_0}-\sin\theta_{1_0})}{r_0^7}\right]\hat{\theta}_2 \\
F_{y2}\,l\,\hat{\theta}_2 = F_{22_0}\,l\,\hat{\theta}_2 &= \left(\frac{-3\mu_0\,\mu^2}{4\pi}\right)\left[-2\,\frac{l\;(l^2\,(1-\cos(\theta_{1_0}-\theta_{2_0}))-2\,a^2)\,(\cos\theta_{2_0}-\cos\theta_{1_0})}{r_0^7}\right]\hat{\theta}_2
\end{aligned} \tag{2.75}$$

Upon substituting the derived linearized expressions for F_{x2} and F_{y2} into the right hand side of the equation of motion we obtain

$$
\begin{aligned}
ml^2\ddot{\hat{\theta}}_2 + c\dot{\hat{\theta}}_2 = &- mg\,l\,\cos\theta_{2_0}\,\hat{\theta}_2 \\
&+ \left(\frac{-3\mu_0\,\mu^2}{4\pi}\right)\left[10\,\frac{l^4\,\left(l^2\left(1-\cos(\theta_{1_0}-\theta_{2_0})\right)-3\,a^2\right)\sin^2(\theta_{1_0}-\theta_{2_0})}{r_0^9}\right. \\
&\qquad\left. -2\,\frac{l^2\,\left(l^2\left(1-\cos(\theta_{1_0}-\theta_{2_0})\right)-2\,a^2\right)\cos(\theta_{1_0}-\theta_{2_0})}{r_0^7}\right]\hat{\theta}_1 \\
&- \left(\frac{-3\mu_0\,\mu^2}{4\pi}\right)\left[10\,\frac{l^4\,\left(l^2\left(1-\cos(\theta_{1_0}-\theta_{2_0})\right)-3\,a^2\right)\sin^2(\theta_{1_0}-\theta_{2_0})}{r_0^9}\right. \\
&\qquad\left. -2\,\frac{l^2\,\left(l^2\left(1-\cos(\theta_{1_0}-\theta_{2_0})\right)-2\,a^2\right)\cos(\theta_{1_0}-\theta_{2_0})}{r_0^7}\right]\hat{\theta}_2 \\
&- \left(\frac{-3\mu_0\,\mu^2}{4\pi}\right)\left[2\,\frac{l^2\,\left(l^2\left(1-\cos(\theta_{1_0}-\theta_{2_0})\right)-2\,a^2\right)\left(\cos\theta_{2_0}-\cos\theta_{1_0}\right)\sin\theta_{2_0}}{r_0^7}\right. \\
&\qquad\left. -2\,\frac{l^2\,\left(l^2\left(1-\cos(\theta_{1_0}-\theta_{2_0})\right)-2\,a^2\right)\left(\sin\theta_{2_0}-\sin\theta_{1_0}\right)\cos\theta_{2_0}}{r_0^7}\right] \\
&- mg\,l\,\sin\theta_{2_0}
\end{aligned}
\tag{2.76}
$$

2.4.5 System Linearized Equations of Motion

Combining the two linearized equations for pendulums 1 and 2 we get (see Eqs. (2.64) and (2.76))

$$
\begin{bmatrix} ml^2 & 0 \\ 0 & ml^2 \end{bmatrix}\begin{bmatrix} \ddot{\hat{\theta}}_1 \\ \ddot{\hat{\theta}}_2 \end{bmatrix} + \begin{bmatrix} c_1 & 0 \\ 0 & c_2 \end{bmatrix}\begin{bmatrix} \dot{\hat{\theta}}_1 \\ \dot{\hat{\theta}}_2 \end{bmatrix} + \begin{bmatrix} k_{11} & k_{12} \\ k_{21} & k_{22} \end{bmatrix}\begin{bmatrix} \hat{\theta}_1 \\ \hat{\theta}_2 \end{bmatrix} = \begin{bmatrix} T_1 \\ T_2 \end{bmatrix} \tag{2.77}
$$

where

$$
\begin{aligned}
k_{11} =& mg\,l\,\cos\theta_{1_0} \\
&+\left(\frac{-3\mu_0\,\mu^2}{4\pi}\right)\left(10\,\frac{l^4\,\left(l^2\,\left(1-\cos\left(\theta_{1_0}-\theta_{2_0}\right)\right)-3\,a^2\right)\sin^2\left(\theta_{1_0}-\theta_{2_0}\right)}{r_0^9}\right. \\
&\qquad\left.-\,2\,\frac{l^2\,\left(l^2\,\left(1-\cos\left(\theta_{1_0}-\theta_{2_0}\right)\right)-2\,a^2\right)\cos\left(\theta_{1_0}-\theta_{2_0}\right)}{r_0^7}\right) \\
k_{22} =& mg\,l\,\cos\theta_{2_0} \\
&+\left(\frac{-3\mu_0\,\mu^2}{4\pi}\right)\left(10\,\frac{l^4\,\left(l^2\,\left(1-\cos\left(\theta_{1_0}-\theta_{2_0}\right)\right)-3\,a^2\right)\sin^2\left(\theta_{1_0}-\theta_{2_0}\right)}{r_0^9}\right. \\
&\qquad\left.-\,2\,\frac{l^2\,\left(l^2\,\left(1-\cos\left(\theta_{1_0}-\theta_{2_0}\right)\right)-2\,a^2\right)\cos\left(\theta_{1_0}-\theta_{2_0}\right)}{r_0^7}\right)
\end{aligned}
\tag{2.78}
$$

$$
\begin{aligned}
k_{12} =& -\left(\frac{-3\mu_0\,\mu^2}{4\pi}\right)\left(10\,\frac{l^4\,\left(l^2\,\left(1-\cos\left(\theta_{1_0}-\theta_{2_0}\right)\right)-3\,a^2\right)\sin^2\left(\theta_{1_0}-\theta_{2_0}\right)}{r_0^9}\right. \\
&\qquad\left.-2\,\frac{l^2\,\left(l^2\,\left(1-\cos\left(\theta_{1_0}-\theta_{2_0}\right)\right)-2\,a^2\right)\cos\left(\theta_{1_0}-\theta_{2_0}\right)}{r_0^7}\right) \\
k_{21} =& -\left(\frac{-3\mu_0\,\mu^2}{4\pi}\right)\left(10\,\frac{l^4\,\left(l^2\,\left(1-\cos\left(\theta_{1_0}-\theta_{2_0}\right)\right)-3\,a^2\right)\sin^2\left(\theta_{1_0}-\theta_{2_0}\right)}{r_0^9}\right. \\
&\qquad\left.-2\,\frac{l^2\,\left(l^2\,\left(1-\cos\left(\theta_{1_0}-\theta_{2_0}\right)\right)-2\,a^2\right)\cos\left(\theta_{1_0}-\theta_{2_0}\right)}{r_0^7}\right)
\end{aligned}
$$

and where

$$
\begin{aligned}
T_1 =& \left(\frac{-3\mu_0\,\mu^2}{4\pi}\right)\left[2\,\frac{l^2\,\left(l^2\left(1-\cos(\theta_{1_0}-\theta_{2_0})\right)-2\,a^2\right)\left(\cos\theta_{2_0}-\cos\theta_{1_0}\right)\sin\theta_{1_0}}{r_0^7}\right. \\
&\qquad\left.-2\,\frac{l^2\,\left(l^2\left(1-\cos(\theta_{1_0}-\theta_{2_0})\right)-2\,a^2\right)\left(\sin\theta_{2_0}-\sin\theta_{1_0}\right)\cos\theta_{1_0}}{r_0^7}\right] \\
&-mg\,l\,\sin\theta_{1_0} \\
T_2 =& -\left(\frac{-3\mu_0\,\mu^2}{4\pi}\right)\left[2\,\frac{l^2\sin\theta_{2_0}\,\left(l^2\left(1-\cos(\theta_{1_0}-\theta_{2_0})\right)-2\,a^2\right)\left(\cos\theta_{2_0}-\cos\theta_{1_0}\right)}{r_0^7}\right. \\
&\qquad\left.-2\,\frac{l^2\cos\theta_{2_0}\,\left(l^2\left(1-\cos(\theta_{1_0}-\theta_{2_0})\right)-2\,a^2\right)\left(\sin\theta_{2_0}-\sin\theta_{1_0}\right)}{r_0^7}\right] \\
&-mg\,l\,\sin\theta_{2_0}
\end{aligned}
\tag{2.79}
$$

Note that Eq. (2.77) can be written as

$$\begin{bmatrix} \ddot{\hat{\theta}}_1 \\ \ddot{\hat{\theta}}_2 \end{bmatrix} + \begin{bmatrix} d_1 & 0 \\ 0 & d_2 \end{bmatrix} \begin{bmatrix} \dot{\hat{\theta}}_1 \\ \dot{\hat{\theta}}_2 \end{bmatrix} + \begin{bmatrix} \alpha_1 & \beta_1 \\ \beta_2 & \alpha_2 \end{bmatrix} \begin{bmatrix} \hat{\theta}_1 \\ \hat{\theta}_2 \end{bmatrix} = \begin{bmatrix} \tau_1 \\ \tau_2 \end{bmatrix} \tag{2.80}$$

where the damping matrix entries are

$$d_1 = \frac{c_1}{ml^2}, \quad \text{and} \quad d_2 = \frac{c_2}{ml^2} \tag{2.81}$$

the stiffness matrix entries are

$$\alpha_1 = \frac{k_{11}}{ml^2}, \quad \beta_1 = \frac{k_{12}}{ml^2}, \quad \beta_2 = \frac{k_{21}}{ml^2}, \quad \text{and} \quad \alpha_2 = \frac{k_{22}}{ml^2} \tag{2.82}$$

and the applied torques are

$$\tau_1 = \frac{T_1}{ml^2}, \quad \text{and} \quad \tau_2 = \frac{T_2}{ml^2} \tag{2.83}$$

Assuming that the pendulums are identical and $c_1 = c_2$ then we can write

$$\begin{aligned}
\alpha_1 =& \frac{g}{l} \cos\theta_{1_0} \\
&+ \left(\frac{-3\mu_0\,\mu^2}{4\,\pi\,m\,l^2}\right)\left(10\,\frac{l^4\,\left(l^2\,\left(1-\cos\left(\theta_{1_0}-\theta_{2_0}\right)\right)-3\,a^2\right)\sin^2\left(\theta_{1_0}-\theta_{2_0}\right)}{r_0^9}\right) \\
&+ \left(\frac{-3\mu_0\,\mu^2}{4\,\pi\,m\,l^2}\right)\left(-2\,\frac{l^2\,\left(l^2\,\left(1-\cos\left(\theta_{1_0}-\theta_{2_0}\right)\right)-2\,a^2\right)\cos\left(\theta_{1_0}-\theta_{2_0}\right)}{r_0^7}\right) \\
\alpha_2 =& \frac{g}{l} \cos\theta_{2_0} \\
&+ \left(\frac{-3\mu_0\,\mu^2}{4\,\pi\,m\,l^2}\right)\left(10\,\frac{l^4\,\left(l^2\,\left(1-\cos\left(\theta_{1_0}-\theta_{2_0}\right)\right)-3\,a^2\right)\sin^2\left(\theta_{1_0}-\theta_{2_0}\right)}{r_0^9}\right) \\
&+ \left(\frac{-3\mu_0\,\mu^2}{4\,\pi\,m\,l^2}\right)\left(-2\,\frac{l^2\,\left(l^2\,\left(1-\cos\left(\theta_{1_0}-\theta_{2_0}\right)\right)-2\,a^2\right)\cos\left(\theta_{1_0}-\theta_{2_0}\right)}{r_0^7}\right)
\end{aligned} \tag{2.84}$$

$$\begin{aligned}
\beta_1 =& -\left(\frac{-3\mu_0\,\mu^2}{4\,\pi\,m\,l^2}\right)\left(10\,\frac{l^4\,\left(l^2\,\left(1-\cos\left(\theta_{1_0}-\theta_{2_0}\right)\right)-3\,a^2\right)\sin^2\left(\theta_{1_0}-\theta_{2_0}\right)}{r_0^9}\right. \\
&\left.-2\,\frac{l^2\,\left(l^2\,\left(1-\cos\left(\theta_{1_0}-\theta_{2_0}\right)\right)-2\,a^2\right)\cos\left(\theta_{1_0}-\theta_{2_0}\right)}{r_0^7}\right) \\
\beta_2 =& -\left(\frac{-3\mu_0\,\mu^2}{4\,\pi\,m\,l^2}\right)\left(10\,\frac{l^4\,\left(l^2\,\left(1-\cos\left(\theta_{1_0}-\theta_{2_0}\right)\right)-3\,a^2\right)\sin^2\left(\theta_{1_0}-\theta_{2_0}\right)}{r_0^9}\right. \\
&\left.-2\,\frac{l^2\,\left(l^2\,\left(1-\cos\left(\theta_{1_0}-\theta_{2_0}\right)\right)-2\,a^2\right)\cos\left(\theta_{1_0}-\theta_{2_0}\right)}{r_0^7}\right)
\end{aligned} \tag{2.85}$$

where we observe that $\beta_1 = \beta_2 = \beta$. The stiffness matrix can therefore be written as

$$\mathbf{K} = \begin{bmatrix} \alpha_1 & \beta \\ \beta & \alpha_2 \end{bmatrix} \tag{2.86}$$

With reference to Eq. (2.80) we assume a solution of the form

$$\boldsymbol{\theta} = \mathrm{e}^{j\Omega t}\mathbf{e} \tag{2.87}$$

where $j = \sqrt{-1}$ is the imaginary number. Then

$$\ddot{\boldsymbol{\theta}} = -\Omega^2\,\mathrm{e}^{j\Omega t}\mathbf{e} = -\Omega^2\,\boldsymbol{\theta} \tag{2.88}$$

so the undamped and unforced form of Eq. (2.80) can be written as

$$\begin{bmatrix} -\Omega^2 & 0 \\ 0 & -\Omega^2 \end{bmatrix} \begin{bmatrix} \hat{\theta}_1 \\ \hat{\theta}_2 \end{bmatrix} + \begin{bmatrix} \alpha_1 & \beta \\ \beta & \alpha_2 \end{bmatrix} \begin{bmatrix} \hat{\theta}_1 \\ \hat{\theta}_2 \end{bmatrix} = \mathbf{0} \tag{2.89}$$

or as

$$\begin{bmatrix} \alpha_1 - \lambda & \beta \\ \beta & \alpha_2 - \lambda \end{bmatrix} \begin{bmatrix} \hat{\theta}_1 \\ \hat{\theta}_2 \end{bmatrix} = \mathbf{0} \tag{2.90}$$

where $\lambda = \Omega^2$. Which is an eigenvalue problem involving only the matrix $\mathbf{K}$. Because of the assumed form of the solution if $\Omega = \sqrt{\lambda}$ is imaginary (*i.e.* of the form $\Omega = \pm j\varpi$) the solution will grow without bound for the negative case where $\Omega = -j\varpi$. Hence our system will be unstable for $\lambda < 0$.

To solve the above equation, the determinant is taken

$$\begin{vmatrix} \alpha_1 - \lambda & \beta \\ \beta & \alpha_2 - \lambda \end{vmatrix} = 0 \tag{2.91}$$

Hence, the eigenvalues of the stiffness matrix are

$$\begin{aligned} \lambda_1 =& \frac{1}{2}(\alpha_1 + \alpha_2) - \frac{1}{2}\sqrt{(\alpha_1 - \alpha_2)^2 + 4\beta^2} \\ \lambda_2 =& \frac{1}{2}(\alpha_1 + \alpha_2) + \frac{1}{2}\sqrt{(\alpha_1 - \alpha_2)^2 + 4\beta^2} \end{aligned} \tag{2.92}$$

2.4.6 Examples and Special Cases

It is worthwhile to consider some special cases.

Case 1: $\theta_{1_0} = \theta_{2_0} = 0$

In this case we have

$$\alpha_1 = \frac{g}{l} - \frac{3\,\mu_0\,\mu^2}{m\,\pi\,a^5}, \quad \alpha_2 = \frac{g}{l} - \frac{3\,\mu_0\,\mu^2}{m\,\pi\,a^5}, \quad \text{and} \quad \beta = \frac{3\,\mu_0\,\mu^2}{m\,\pi\,a^5} \tag{2.93}$$

which lead to

$$\begin{aligned} \lambda_1 &= \frac{g}{l} - \frac{6\,\mu_0\,\mu^2}{m\,\pi\,a^5} \\ \lambda_2 &= \frac{g}{l} \end{aligned} \tag{2.94}$$

Observe that $\lambda_2 > 0$ and that λ_1 may be positive, negative or zero. The latter case occurs when

$$a = \sqrt[5]{\frac{6\,\mu_0\,\mu^2\,l}{\pi\,mg}} = a_0 \tag{2.95}$$

When $a < a_0$ the system will be unstable because the repulsive magnetic force will dominate over the gravitational force and a small perturbation from $\theta_{1_0} = \theta_{2_0} = 0$ will result in the pendulums moving toward another equilibrium point due to the magnetic repulsion. If $a > a_0$ the system will be stable because the pendulums are too far apart for the magnetic force between them to have a sufficiently strong effect and the gravity force dominates and provides a restorative force that when the system is slightly perturbed in returns to $\theta_{1_0} = \theta_{2_0} = 0$. The eigenvalues proportion for different distances between the two pendulums for both attraction and repulsion is shown in Fig. 2.3 (using the parameter values from Table 4.1 in Chapter 4 resulted in $a_0 = 0.0582$ m).

Case 2: $\theta_{1_0} = 0$, $\theta_{2_0} = \pi$

In this case pendulum number 1 is hanging downward and pendulum number 2 is inverted. The system parameters are

$$\begin{aligned} \alpha_1 &= \frac{g}{l} + \left(\frac{-3\mu_0\,\mu^2}{4\,\pi\,m\,l^2}\right)\frac{4\,l^2\,(l^2 - a^2)}{(4\,l^2 + a^2)^{7/2}} \\ \alpha_2 &= -\frac{g}{l} + \left(\frac{-3\mu_0\,\mu^2}{4\,\pi\,m\,l^2}\right)\frac{4l^2\,(l^2 - a^2)}{(4\,l^2 + a^2)^{7/2}} \\ \beta &= -\left(\frac{-3\mu_0\,\mu^2}{4\,\pi\,m\,l^2}\right)\frac{4\,l^2\,(l^2 - a^2)}{(4\,l^2 + a^2)^{7/2}} \end{aligned} \tag{2.96}$$

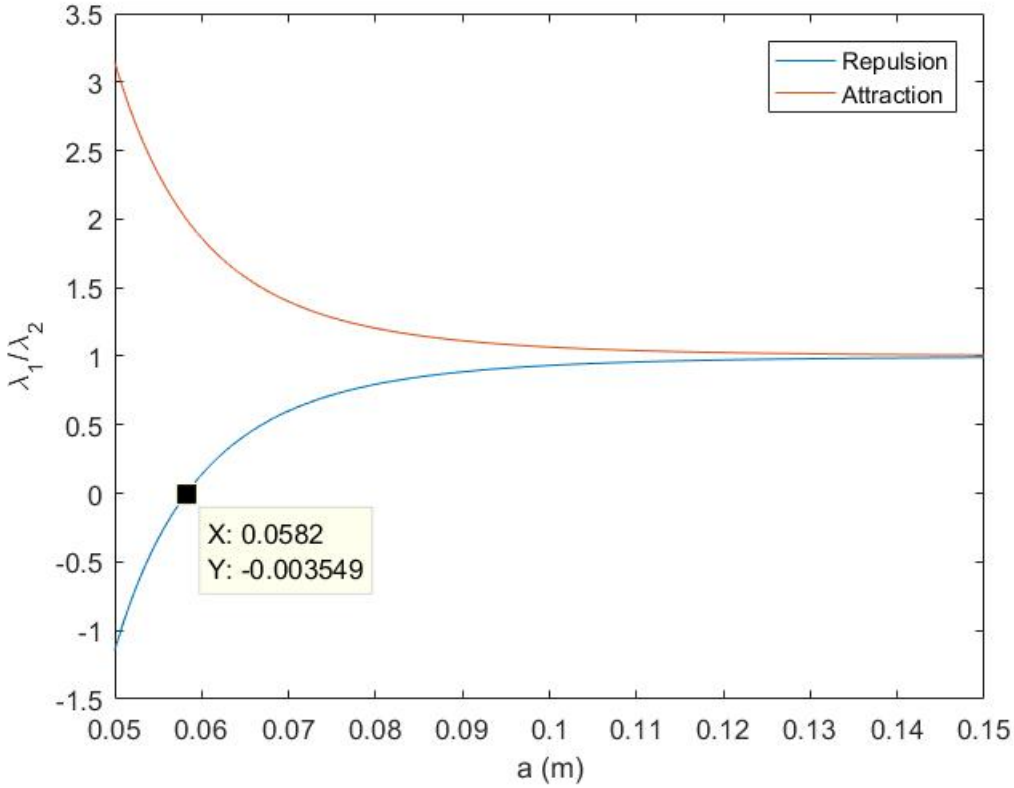

Figure 2.3: Eigenvalues proportion for Case 1 where $\theta_{1_0} = \theta_{2_0} = 0$ for both repulsion and attraction.

which lead to

$$\begin{aligned}
\lambda_1 &= \left(\frac{-3\mu_0\,\mu^2}{4\,\pi\,m\,l^2}\right)\left[\frac{4\,l^2\,(l^2-a^2)}{(4\,l^2+a^2)^{7/2}} + \sqrt{\left(\frac{4\pi\,mg\,l}{3\mu_0\,\mu^2}\right)^2 + \left(\frac{4\,l^2\,(a^2-l^2)}{(4\,l^2+a^2)^{7/2}}\right)^2}\right] \\
\lambda_2 &= \left(\frac{-3\mu_0\,\mu^2}{4\,\pi\,m\,l^2}\right)\left[\frac{4\,l^2\,(l^2-a^2)}{(4\,l^2+a^2)^{7/2}} - \sqrt{\left(\frac{4\pi\,mg\,l}{3\mu_0\,\mu^2}\right)^2 + \left(\frac{4\,l^2\,(a^2-l^2)}{(4\,l^2+a^2)^{7/2}}\right)^2}\right]
\end{aligned} \tag{2.97}$$

The first term in the square brackets of each of λ_1 and λ_2 is always positive and the second term is always larger than the first so that $\lambda_1 < 0$ always and this configuration is unstable as expected.

Case 3: $\theta_{1_0} = \pi$, $\theta_{2_0} = 0$

In this case pendulum number 2 is hanging downward and pendulum number 1 is inverted. The system parameters are

$$\begin{aligned} \alpha_1 &= -\frac{g}{l} + \left(\frac{-3\mu_0\,\mu^2}{4\,\pi\,m\,l^2}\right)\frac{4l^2\,(l^2-a^2)}{(4\,l^2+a^2)^{7/2}} \\ \alpha_2 &= \frac{g}{l} + \left(\frac{-3\mu_0\,\mu^2}{4\,\pi\,m\,l^2}\right)\frac{4\,l^2\,(l^2-a^2)}{(4\,l^2+a^2)^{7/2}} \\ \beta &= -\left(\frac{-3\mu_0\,\mu^2}{4\,\pi\,m\,l^2}\right)\frac{4\,l^2\,(l^2-a^2)}{(4\,l^2+a^2)^{7/2}} \end{aligned} \tag{2.98}$$

which lead to

$$\begin{aligned} \lambda_1 &= \left(\frac{-3\mu_0\,\mu^2}{4\,\pi\,m\,l^2}\right)\left[\frac{4\,l^2\,(l^2-a^2)}{(4\,l^2+a^2)^{7/2}} + \sqrt{\left(\frac{4\pi\,mg\,l}{3\mu_0\,\mu^2}\right)^2 + \left(\frac{4\,l^2\,(a^2-l^2)}{(4\,l^2+a^2)^{7/2}}\right)^2}\right] \\ \lambda_2 &= \left(\frac{-3\mu_0\,\mu^2}{4\,\pi\,m\,l^2}\right)\left[\frac{4\,l^2\,(l^2-a^2)}{(4\,l^2+a^2)^{7/2}} - \sqrt{\left(\frac{4\pi\,mg\,l}{3\mu_0\,\mu^2}\right)^2 + \left(\frac{4\,l^2\,(a^2-l^2)}{(4\,l^2+a^2)^{7/2}}\right)^2}\right] \end{aligned} \tag{2.99}$$

The eigenvalues in this case are, as should be expected, the same as in Case 2 where the first term in each of λ_1 and λ_2 is always positive and the second term is always larger than the first so that $\lambda_1 < 0$ always and this configuration is unstable as expected.

Case 4: $\theta_{1_0} = \pi$, $\theta_{2_0} = \pi$

In this case we have

$$\begin{aligned} \alpha_1 &= -\frac{g}{l} + \left(\frac{-3\mu_0\,\mu^2}{4\,\pi\,m\,l^2}\right)\frac{4\,l^2}{a^5} \\ \alpha_2 &= -\frac{g}{l} + \left(\frac{-3\mu_0\,\mu^2}{4\,\pi\,m\,l^2}\right)\frac{4\,l^2}{a^5} \\ \beta &= -\left(\frac{-3\mu_0\,\mu^2}{4\,\pi\,m\,l^2}\right)\frac{4\,l^2}{a^5} \end{aligned} \tag{2.100}$$

which lead to

$$\begin{aligned}\lambda_1 =& -\frac{g}{l} - \left(\frac{3\mu_0\,\mu^2}{4\,\pi\,m\,l^2}\right)\left(\frac{8\,l^2}{a^5}\right)\\ \lambda_2 =& -\frac{g}{l}\end{aligned} \tag{2.101}$$

Here, both eigenvalues are always negative and the system is unstable.

Case 5: $\theta_{1_0} = \theta$**,** $\theta_{2_0} = -\theta$

In this case we examine the situation where $\theta_{1_0} = -\theta_{2_0}$ which is the remaining possible equilibrium configuration. For this arrangement

$$\begin{aligned}\alpha_1 =& \frac{g}{l}\,\cos\theta\\ &+\left(\frac{-3\mu_0\,\mu^2}{4\,\pi\,m\,l^2}\right)\left(10\,\frac{l^4\,\left(l^2\,\left(1-\cos\left(2\theta\right)\right)-3\,a^2\right)\sin^2\left(2\theta\right)}{r_0^9}\right)\\ &+\left(\frac{-3\mu_0\,\mu^2}{4\,\pi\,m\,l^2}\right)\left(-2\,\frac{l^2\,\left(l^2\,\left(1-\cos\left(2\theta\right)\right)-2\,a^2\right)\cos\left(2\theta\right)}{r_0^7}\right)\\ \alpha_2 =& \frac{g}{l}\,\cos\theta\\ &+\left(\frac{-3\mu_0\,\mu^2}{4\,\pi\,m\,l^2}\right)\left(10\,\frac{l^4\,\left(l^2\,\left(1-\cos\left(2\theta\right)\right)-3\,a^2\right)\sin^2\left(2\theta\right)}{r_0^9}\right)\\ &+\left(\frac{-3\mu_0\,\mu^2}{4\,\pi\,m\,l^2}\right)\left(-2\,\frac{l^2\,\left(l^2\,\left(1-\cos\left(2\theta\right)\right)-2\,a^2\right)\cos\left(2\theta\right)}{r_0^7}\right)\end{aligned} \tag{2.102}$$

$$\begin{aligned}\beta = \left(\frac{3\mu_0\,\mu^2}{4\,\pi\,m\,l^2}\right)\Bigg(&10\,\frac{l^4\,\left(l^2\,\left(1-\cos\left(2\theta\right)\right)-3\,a^2\right)\sin^2\left(2\theta\right)}{r_0^9}\\ &-2\,\frac{l^2\,\left(l^2\,\left(1-\cos\left(2\theta\right)\right)-2\,a^2\right)\cos\left(2\theta\right)}{r_0^7}\Bigg)\end{aligned} \tag{2.103}$$

where, for this set of θ_{1_0} and θ_{2_0}

$$r_{01} = r_{02} = \sqrt{2\,l^2(1-\cos(2\,\theta)) + a^2} \tag{2.104}$$

which upon noticing that $\alpha_1 = \alpha_2$ substitution gives

$$\lambda_1 = \alpha_1 - \beta \quad \text{and} \quad \lambda_2 = \alpha_1 + \beta \tag{2.105}$$

or, in more detail,

$$\begin{aligned}\lambda_1 =& \frac{g}{l}\,\cos\theta \\ &+\left(\frac{-6\mu_0\,\mu^2}{4\,\pi\,m\,l^2}\right)\left(10\,\frac{l^4\,\left(l^2\,\left(1-\cos\left(2\theta\right)\right)-3\,a^2\right)\sin^2\left(2\theta\right)}{r_0^9}\right. \\ &\qquad\left.-2\,\frac{l^2\,\left(l^2\,\left(1-\cos\left(2\theta\right)\right)-2\,a^2\right)\cos\left(2\theta\right)}{r_0^7}\right) \\ \lambda_2 =& \frac{g}{l}\,\cos\theta\end{aligned} \tag{2.106}$$

Clearly $\lambda_2 > 0$ because $\theta < 90°$, but λ_1 is not necessarily always positive. As it is shown in Fig. 2.4, for large enough values of a this configuration will be stable ($\lambda_1 > 0$) but for small values of a it will not be stable ($\lambda_1 < 0$). It is worthwhile to note that the small region of instability for small values of a arises because in that region the torque due to gravity cannot balance what becomes very large magnetic torques and the identified equilibrium angle cannot be stable for very small values of a (using the parameter values from Table 4.1 in Chapter 4 represents that for $a > 0.0127$ m the system is stable and it confirms the experiment where $a = 0.041$ m).

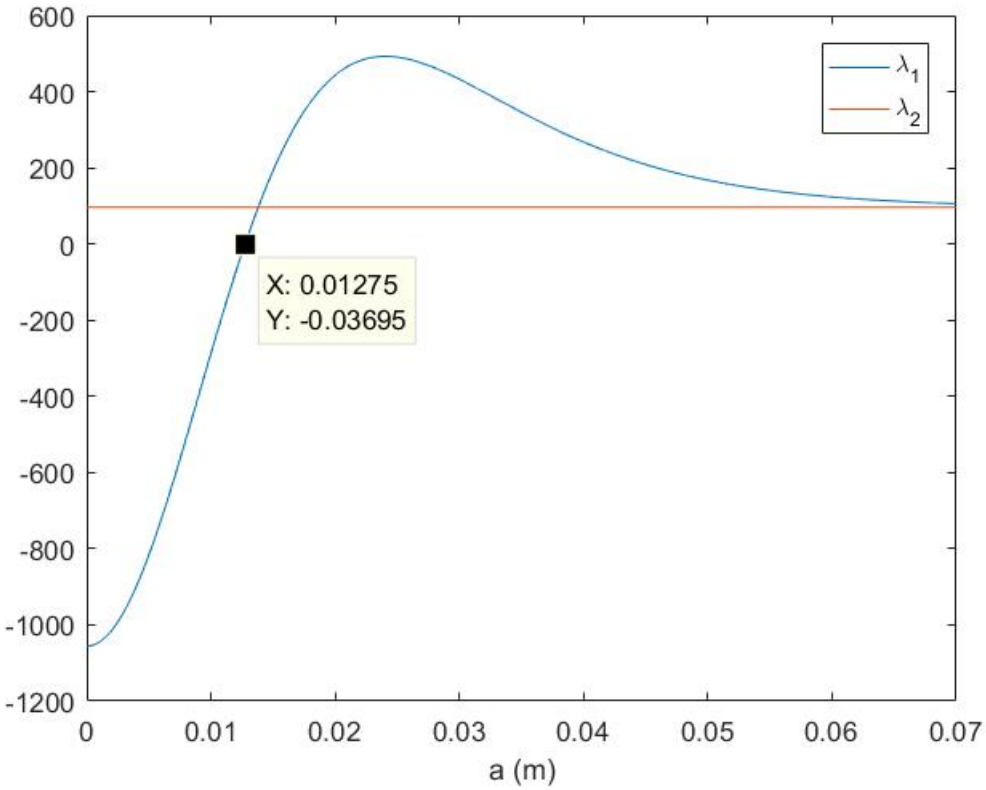

Figure 2.4: Eigenvalues for Case 5 where $\theta_{1_0} = \theta$, $\theta_{2_0} = -\theta$.

2.5 Rigid Body Model of a Pendulum

Consider a series of N pendulums as described in section 2.1. All the properties including a fixed inertial frame and the distance between the pendulums are the same but in this section each pendulum is considered to be rigid body of mass m_i and mass moment of inertia of J_i, $i = 1, 2, \cdots N$. The length of each pendulum is l_i and the distance between origin O_i and the center of mass, G_i, is denoted as d_i. Again the single degree of freedom of each pendulum is the angle it makes with the vertical direction and these angles are denoted as θ_i. In this case the gravitational forces are acting on the pendulum's center of mass rather than the magnet. But the position of the magnetic forces are still the same. The location of the forces for pendulum i is illustrated in Fig. 2.5. It should be noted that the magnetic force acting on dipole i due to magnetic dipole j is not changed and can be calculated from Eq. (2.23), because the magnets used in this model are identical with the ones in the ideal point mass model.

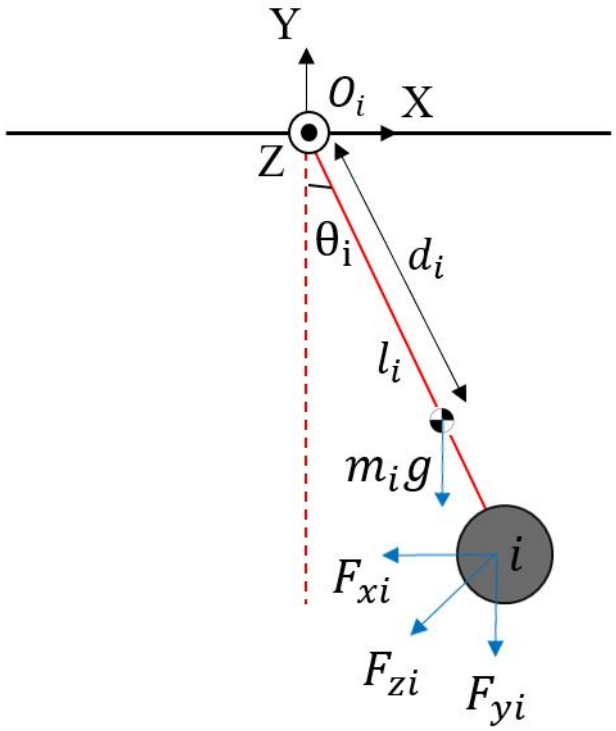

Figure 2.5: Side view of the rigid body model.

There is a gravitational force of the form

$$\boldsymbol{F}_{gi} = \begin{bmatrix} 0 \\ -m_i g \\ 0 \end{bmatrix} \tag{2.107}$$

where m_i is considered to be the total mass of the pendulum i, including the rod and the magnet.

Both the magnetic and the gravitational forces will generate moments about the point of suspension of each pendulum.The moment about O_i is given by

$$\vec{M}_i = \vec{r}_{Oi} \times \vec{F}_{mi} + \vec{r}_{Gi} \times \vec{F}_{gi} \tag{2.108}$$

Where the position of the magnet i is defined by the position vector $\vec{r}_{Oi}$, which extends from the point of suspension of the pendulum, O_i, to the magnet and the position of pendulum i's center of mass is defined by the position vector $\vec{r}_{Gi}$, which extends from O_i to the pendulum's center of mass. From Fig. 2.5

$$\boldsymbol{r}_{Oi} = \begin{bmatrix} l_i \sin\theta_i \\ -l_i \cos\theta_i \\ 0 \end{bmatrix} \tag{2.109}$$

and

$$\boldsymbol{r}_{Gi} = \begin{bmatrix} d_i \sin\theta_i \\ -d_i \cos\theta_i \\ 0 \end{bmatrix} \tag{2.110}$$

and hence from Eq. (2.108)

$$\begin{aligned} \boldsymbol{M}_i &= \begin{bmatrix} l_i \sin\theta_i \\ -l_i \cos\theta_i \\ 0 \end{bmatrix} \times \begin{bmatrix} F_{xi} \\ F_{yi} \\ F_{zi} \end{bmatrix} + \begin{bmatrix} d_i \sin\theta_i \\ -d_i \cos\theta_i \\ 0 \end{bmatrix} \times \begin{bmatrix} 0 \\ -m_i g \\ 0 \end{bmatrix} \\ &= \begin{bmatrix} -F_{zi}(l_i \cos\theta_i) \\ -F_{zi}(l_i \sin\theta_i) \\ (F_{yi} - m_i g)(l_i \sin\theta_i) + F_{xi}(l_i \cos\theta_i) - m_i g(d_i \sin\theta_i) \end{bmatrix} \end{aligned} \tag{2.111}$$

In addition to the moments that arise due to magnetic forces and gravity there will also be reaction moments (torques) at the suspension point. These are assumed to be of the form

$$\boldsymbol{M}_{Ri} = \begin{bmatrix} T_{xi} \\ T_{yi} \\ -c_i \dot{\theta}_i \end{bmatrix} \tag{2.112}$$

where T_{xi} is the twisting moment about the X axis, T_{yi} is the bending moment about the Y axis and $-c\dot{\theta}_i$ is the viscous damping moment acting about the Z axis.

Euler's equation for the motion of pendulum i is

$$\vec{J}_i \,.\, \vec{\alpha}_i + \vec{\omega}_i \times \vec{J}_i \,.\, \vec{\omega}_i = \vec{M}_i + \vec{M}_{Ri} \tag{2.113}$$

where $\vec{J}_i$ is the inertia dyadic of pendulum i which is expressed in the form of

$$\boldsymbol{J}_i = \begin{bmatrix} J_{xx} & J_{xy} & J_{xz} \\ J_{yx} & J_{yy} & J_{yz} \\ J_{zx} & J_{zy} & J_{zz} \end{bmatrix} \tag{2.114}$$

Further, with respect to Eq. (2.113), we have that

$$\boldsymbol{\alpha}_i = \begin{bmatrix} 0 \\ 0 \\ \ddot{\theta}_i \end{bmatrix} \quad \text{and} \quad \boldsymbol{\omega}_i = \begin{bmatrix} 0 \\ 0 \\ \dot{\theta}_i \end{bmatrix} \tag{2.115}$$

where $\vec{\alpha}$ is the angular acceleration and $\vec{\omega}$ is the angular velocity.

Substituting Eq. (2.114) and Eq. (2.115) into Eq. (2.113) gives us

$$\begin{bmatrix} J_{xz}\ddot{\theta}_i - J_{yz}\dot{\theta}_i^{\,2} \\ J_{yz}\ddot{\theta}_i + J_{xz}\dot{\theta}_i^{\,2} \\ J_{zz}\ddot{\theta}_i \end{bmatrix} = \boldsymbol{M}_i + \boldsymbol{M}_{Ri} \tag{2.116}$$

So the governing equation for pendulum i, is

$$\begin{bmatrix} J_{xz}\ddot{\theta}_i - J_{yz}\dot{\theta}_i^{\,2} \\ J_{yz}\ddot{\theta}_i + J_{xz}\dot{\theta}_i^{\,2} \\ J_{zz}\ddot{\theta}_i \end{bmatrix} = \begin{bmatrix} -F_{zi}(l_i \cos\theta_i) \\ -F_{zi}(l_i \sin\theta_i) \\ (F_{yi} - m_i g)(l_i \sin\theta_i) + F_{xi}(l_i \cos\theta_i) - m_i g(d_i \sin\theta_i) \end{bmatrix} + \begin{bmatrix} T_{xi} \\ T_{yi} \\ -c_i\dot{\theta}_i \end{bmatrix} \tag{2.117}$$

From these we can see that $T_{xi} = F_{zi}(l_i \cos\theta_i) + J_{xz}\ddot{\theta}_i - J_{yz}\dot{\theta}_i^{\,2}$ is twisting reaction at the suspension point and $T_{yi} = F_{zi}(l_i \sin\theta_i) + J_{yz}\ddot{\theta}_i + J_{xz}\dot{\theta}_i^{\,2}$ is the time dependent bending moment at the suspension point.

2.6 Special Case: $N = 2$, Repulsion

Again we will consider the special case of two identical pendulums where the magnets are arranged so that there is a repulsive force between them. This time the rigid body case is

investigated. We shall simplify the governing equations using the following substitutions:

$$\begin{aligned} B_{r1} &= B_{r2} = B_r \\ c_1 &= c_2 = c \\ l_1 &= l_2 = l \\ d_1 &= d_2 = d \\ m_1 &= m_2 = m \\ J_1 &= J_2 = J \\ M_1 &= M_2 = M \\ V_1 &= V_2 = V \\ z_1 &= 0, \qquad z_2 = \ a \\ \mu_1 &= \mu, \qquad \mu_2 = -\mu \end{aligned} \tag{2.118}$$

Note that the last two assumptions mean that the north poles of the two magnets are facing one another.

2.6.1 Pendulum 1: General Equations of Motion

The governing equations for pendulum 1 are (from Eq. (2.117))

$$\begin{bmatrix} J_{xz}\ddot{\theta}_1 - J_{yz}\dot{\theta}_1^{\,2} \\ J_{yz}\ddot{\theta}_1 + J_{xz}\dot{\theta}_1^{\,2} \\ J_{zz}\ddot{\theta}_1 \end{bmatrix} = \begin{bmatrix} -F_{z1}(l\cos\theta_1) \\ -F_{z1}(l\sin\theta_1) \\ (F_{y1} - mg)(l\sin\theta_1) + F_{x1}(l\cos\theta_1) - mg(d\sin\theta_1) \end{bmatrix} + \begin{bmatrix} T_{x1} \\ T_{y1} \\ -c\dot{\theta}_1 \end{bmatrix} \tag{2.119}$$

To find the Euler equation we will need $\vec{F}_{m1}$. Where, from Eq. (2.23), (remember that $\mu_1 = \mu$ and $\mu_2 = -\mu$)

$$\boldsymbol{F}_{m1} = \begin{bmatrix} F_{x1} \\ F_{y1} \\ F_{z1} \end{bmatrix} = \frac{3\mu_0\mu^2}{4\pi} \begin{bmatrix} \frac{5x_{12}z_{12}^2}{r_{12}^7} - \frac{x_{12}}{r_{12}^5} \\ \frac{5y_{12}z_{12}^2}{r_{12}^7} - \frac{y_{12}}{r_{12}^5} \\ \frac{5z_{12}^3}{r_{12}^7} - \frac{3z_{12}}{r_{12}^5} \end{bmatrix} \tag{2.120}$$

Recall from Eq. (2.6)

$$\boldsymbol{r}_{12} = \begin{bmatrix} x_{12} \\ y_{12} \\ z_{12} \end{bmatrix} = \begin{bmatrix} l\sin\theta_1 - l\sin\theta_2 \\ -l\cos\theta_1 + l\cos\theta_2 \\ -a \end{bmatrix} \tag{2.121}$$

and from Eq. (2.8)

$$r_{12} = \sqrt{(l\sin\theta_1 - l\sin\theta_2)^2 + (-l\cos\theta_1 + l\cos\theta_2)^2 + a^2} = \sqrt{a^2 + 2l^2(1-\cos(\theta_2-\theta_1))} \tag{2.122}$$

Also, from Eq. (2.107)

$$\boldsymbol{F}_{g1} = \begin{bmatrix} 0 \\ -mg \\ 0 \end{bmatrix} \tag{2.123}$$

and therefore Euler's equation for θ_1 (from Eq. (2.119)) is

$$J_{zz}\ddot{\theta}_1 = F_{y1}(l\sin\theta_1) + F_{x1}(l\cos\theta_1) - mg(d\sin\theta_1) - c\dot{\theta}_1 \tag{2.124}$$

which is the complete nonlinear equation of motion for pendulum 1. Divide through by J_{zz} to find

$$\ddot{\theta}_1 + \left(\frac{c}{J_{zz}}\right)\dot{\theta}_1 - \left(\frac{F_{y1}l}{J_{zz}} - \frac{mgd}{J_{zz}}\right)\sin\theta_1 - \left(\frac{F_{x1}l}{J_{zz}}\right)\cos\theta_1 = 0 \tag{2.125}$$

2.6.2 Pendulum 2: General Equations of Motion

The governing equations for pendulum 2 are (from Eq. (2.117))

$$\begin{bmatrix} J_{xz}\ddot{\theta}_2 - J_{yz}\dot{\theta}_2^{\,2} \\ J_{yz}\ddot{\theta}_2 + J_{xz}\dot{\theta}_2^{\,2} \\ J_{zz}\ddot{\theta}_2 \end{bmatrix} = \begin{bmatrix} -F_{z2}(l\cos\theta_2) \\ -F_{z2}(l\sin\theta_2) \\ (F_{y2}-mg)(l\sin\theta_2) + F_{x2}(l\cos\theta_2) - mg(d\sin\theta_2) \end{bmatrix} + \begin{bmatrix} T_{x2} \\ T_{y2} \\ -c\dot{\theta}_2 \end{bmatrix} \tag{2.126}$$

To find the Euler equation we will need $\vec{F}_{m2}$. Where, from Eq. (2.23), (remember that $\mu_1 = \mu$ and $\mu_2 = -\mu$)

$$\boldsymbol{F}_{m2} = \begin{bmatrix} F_{x2} \\ F_{y2} \\ F_{z2} \end{bmatrix} = \frac{3\mu_0\mu^2}{4\pi}\begin{bmatrix} \frac{5x_{21}z_{21}^2}{r_{21}^7} - \frac{x_{21}}{r_{21}^5} \\ \frac{5y_{21}z_{21}^2}{r_{21}^7} - \frac{y_{21}}{r_{21}^5} \\ \frac{5z_{21}^3}{r_{21}^7} - \frac{3z_{21}}{r_{21}^5} \end{bmatrix} \tag{2.127}$$

Recall from Eq. (2.6)

$$\boldsymbol{r}_{21} = \begin{bmatrix} x_{21} \\ y_{21} \\ z_{21} \end{bmatrix} = \begin{bmatrix} l\sin\theta_2 - l\sin\theta_1 \\ -l\cos\theta_2 + l\cos\theta_1 \\ -a \end{bmatrix} \tag{2.128}$$

and from Eq. (2.8)

$$r_{21} = \sqrt{(l\sin\theta_2 - l\sin\theta_1)^2 + (-l\cos\theta_2 + l\cos\theta_1)^2 + a^2} = \sqrt{a^2 + 2l^2(1-\cos(\theta_2-\theta_1))} \tag{2.129}$$

The gravity force vector $\vec{F}_{g2} = \vec{F}_{g1}$ as given in Eq. (2.123) and therefore Euler's equation for θ_2 (from Eq. (2.119)) is

$$J_{zz}\ddot{\theta}_2 = F_{y2}(l\sin\theta_2) + F_{x1}(l\cos\theta_2) - mg(d\sin\theta_2) - c\dot{\theta}_2 \tag{2.130}$$

which is the complete nonlinear equation of motion for pendulum 2. Divide through by J_{zz} to find

$$\ddot{\theta}_2 + \left(\frac{c}{J_{zz}}\right)\dot{\theta}_2 - \left(\frac{F_{y2}l}{J_{zz}} - \frac{mgd}{J_{zz}}\right)\sin\theta_2 - \left(\frac{F_{x2}l}{J_{zz}}\right)\cos\theta_2 = 0 \tag{2.131}$$

Chapter 3

Experiment Design

We are seeking to analyze the behaviour of the system experimentally to investigate how accurate our analytical approach is. In order to reach this objective, a simple experimental setup composed of an array of coupled magnetic pendulums is proposed. In this chapter the procedure of experiment design is presented.

This chapter is organized as follows: in section 3.1 the design steps of the experiment required parts are described. Section 3.2 covers the theoretical calculations of designing the pendulum in detail and finally, the suspension rod design is presented in section 3.3.

3.1 Design Steps

A pair of coaxial coupled magnetic pendulums was to be built, where the magnets were to be oriented such that there would be either a repulsive force between them or, by mounting one magnet the other way around, an attractive force between them. The first pendulum would be released from a specific angle and both pendulums were to be allowed to oscillate freely. The motion of the pair was to be recorded using a camera.

The first step was selecting the proper magnet. A magnet that was strong compared to its size was desired so that the pendulums could be strongly coupled. The DA2-N52 magnet from K&J Magnetics [18] was chosen as a representative magnet. The magnet's parameter values are given in Table 3.1.

The length of the pendulum was chosen to be $l = 10$ cm to allow the motion of the pendulum to be readily observable but to also limit the bending that could occur due to the magnetic forces between pendulums.

Table 3.1: Dimensions and parameter values for the DA2-N52 magnet.

Description	Symbol	Value [US]	Value [SI]
DA2-N52 magnet diameter	D	0.625 in	1.5875 cm
DA2-N52 magnet thickness	h	0.125 in	0.3175 cm
DA2-N52 magnet volume	$V = \pi \frac{D^2}{4} h$	3.84×10^{-2} in^3	0.628 cm^3
DA2-N52 magnet mass	m_m	0.166 oz	4.71 g
DA2-N52 magnet residual flux density	B_r		1.48 Tesla
DA2-N52 magnet Magnetization	$M = \frac{B_r}{\mu_0}$		11.77×10^5 A/m

Table 3.2: Dimensions and parameter values for the deep groove ball bearing.

Description	Symbol	Value [SI]
Bearing inner diameter	D_{bi}	5 mm
Bearing outer diameter	D_{bo}	16 mm
Bearing thickness	h_b	5 mm
Bearing mass	m_b	0.57 g

The second step was designing the pendulums. A pendulum body should have low weight and hence, be comparable to the ideal point mass model. However, it should also be stiff so it will not bend due to the magnetic forces.

The third step was choosing an appropriate suspension rod to attach the pendulums to. The deflection of the rod was calculated assuming that it was loaded by the weight of eight equally spaced identical pendulums. As a result of this calculation 5 mm oil hardened drill rod was selected [19].

Furthermore, a ball bearing with low friction and suitable size was needed. A deep groove ball bearing from Bearings Canada [20] was chosen. The bearing dimensions are given in Table 3.2.

Table 3.3: Dimensions and parameter values for the pendulum design.

Description	Symbol	Value [US]	Value [SI]
Acceleration due to gravity	g	32.17 ft/s^2	9.804 m/s^2
Permeability of free space	μ_0		$4\pi \times 10^{-7}$ H·m^{-1}
Pendulum magnet separation	a		3.7 cm
Pendulum length	l		10 cm
Pendulum body thickness	t	0.375 in	9.525 mm
Pendulum mass	m_p		10.07 g
PMMA density	ρ		1.17 g/cm^3
PMMA ultimate strength	σ_u		70 MPa

3.2 Pendulum Design

To design a pendulum, a lightweight material was chosen in order that the resulting pendulum could be considered to be close to the ideal point mass model, where only the mass of the magnet is significant and the pendulum body weight could be considered to be negligible. The material which has been selected is Poly(methyl methacrylate)(PMMA), it is also known as plexiglass. The PMMA material properties are given in Table 3.3.

Then we had to make sure that the PMMA could withstand the magnetic forces applied to the pendulum and that it would not bend significantly. To investigate this, the maximum stress on pendulum should have been less than the ultimate strength of PMMA *i.e.* $\sigma_{max} < \sigma_U$. The experimental setup is shown in Fig. 3.1.

Maximum stress is applied where the pendulums are attached to a rigid bar and it can be calculated from

$$\sigma_{max} = \frac{T_x c}{I} \tag{3.1}$$

where T_x is the bending moment about the X-axis at the location of interest along the beam's length, I is the centroidal moment of inertia of the pendulum body's cross section and c is the distance from the centroidal axis to the extreme fiber of the pendulum.

A schematic side view of the pendulum and cross section of that is depicted in Fig. 3.2 and $c = t/2$ where t is the pendulum thickness.

Taking the cross section of the pendulum body to be rectangular the centroidal moment

Figure 3.1: Experimental setup for two magnetic pendulums.

of inertia can be determined using

$$I = \frac{1}{12} w t^3 - \frac{1}{12} D_{bo} t^3 \tag{3.2}$$

where w is a width of pendulum at the suspension point and D_{bo} is the bearing outer diameter (see Fig. 3.2).

The maximum bending moment at the suspension point due to the magnetic force acting on the pendulum, T_x, can be found using Eq. (2.111) to be

$$T_x = F_{z1} l \tag{3.3}$$

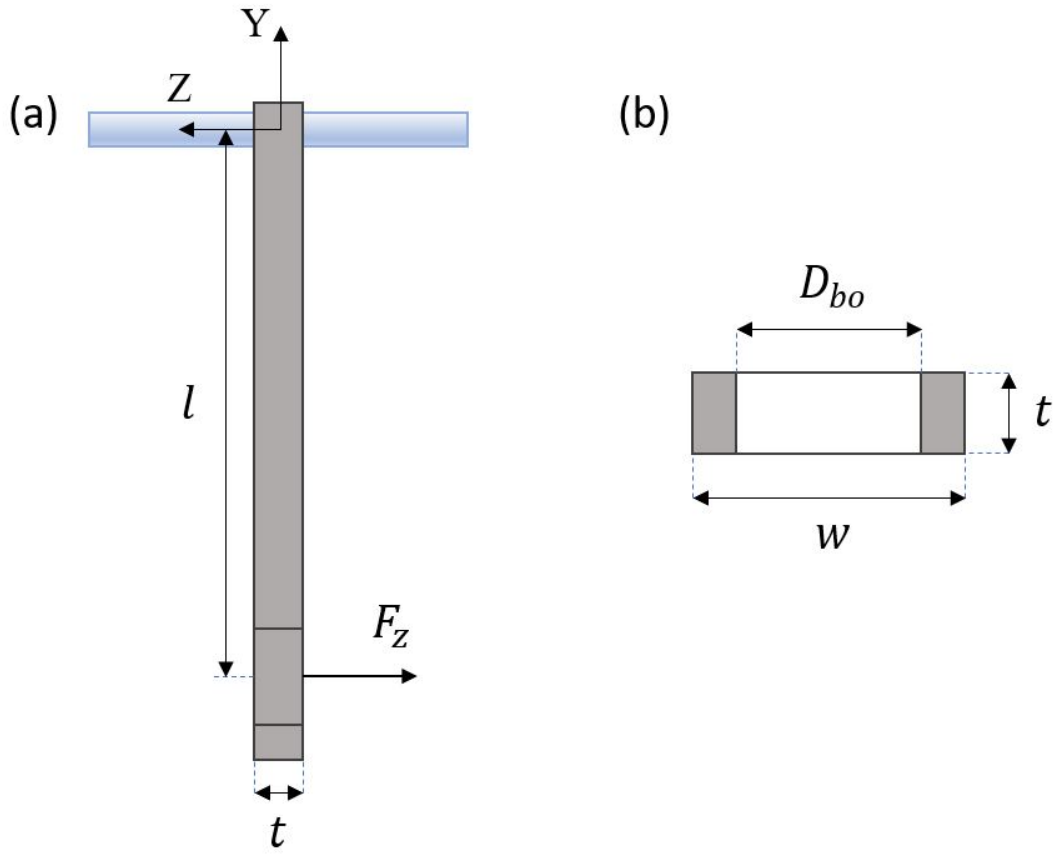

Figure 3.2: Schematic diagram of the pendulum: (a) Side view of the pendulum, (b) Cross section of the pendulum at the suspension point.

From Eq. (2.120), the magnetic force along the rod direction, F_{z1}, is given by

$$F_{z1} = \frac{3\mu_0\mu^2}{4\pi}\left(\frac{5z_{12}^3}{r_{12}^7} - \frac{3z_{12}}{r_{12}^5}\right) \tag{3.4}$$

and recall from Eq. (2.121) that

$$z_{12} = -a \tag{3.5}$$

as well as that the magnitude of $\vec{r}_{12}$ from Eq. (2.122) is

$$r_{12} = \sqrt{a^2 + 2l^2(1 - \cos(\theta_2 - \theta_1))} \tag{3.6}$$

The magnetic force F_{z1} is maximum when the two pendulums are crossing one another *i.e.* when $\theta_1 = \theta_2$. By substituting $\theta_1 = \theta_2$ in Eq. (3.6), the magnitude of $\vec{r}_{12}$ becomes

$$r_{12} = a \tag{3.7}$$

then making the replacements Eq. (3.5) and Eq. (3.7) in Eq. (3.4) yields

$$F_{z1} = \frac{-3\mu_0\mu^2}{2\pi a^4} \tag{3.8}$$

Recall from Eq. (2.2)

$$\vec{\mu} = \frac{\vec{B}_r V}{\mu_0} \tag{3.9}$$

where $\vec{B}_r$ is the magnet's residual flux density (Tesla= $\frac{Wb}{m^2}$), V is the magnet's volume, and μ_0 is the permeability of free space. Hence Eq. (3.8) can be rewritten in the form of

$$F_{z1} = \frac{-3B_r^2V^2}{2\pi\mu_0 a^4} \tag{3.10}$$

Therefore, by using Eq. (3.10) in Eq. (3.3), the bending moment at the suspension point, T_x, is given by

$$T_x = \frac{-3B_r^2V^2 l}{2\pi\mu_0 a^4} \tag{3.11}$$

Finally, a maximum stress, σ_{max}, can be determined by substituting Eq. (3.2) and Eq. (3.11) into Eq. (3.1).

The maximum stress which is found should be significantly lower than the ultimate strength of PMMA, *i.e.* $\sigma_{max} < \sigma_U$, to guarantee that a pendulum will not fail due to the magnetic forces and the design is acceptable.

Now let's find the maximum stress for our specific experiment. The DA2-N52 neodymium magnet has a diameter $D = 1.5875$ cm, a thickness $h = 0.3175$ cm, and a residual flux density $B_r = 1.48$ Tesla. The volume of the magnet, V, can be determined using

$$V = \frac{\pi D^2 h}{4} \tag{3.12}$$

Hence, the volume of the magnet is going to be $V = 0.628 \times 10^{-6}$ m^3.

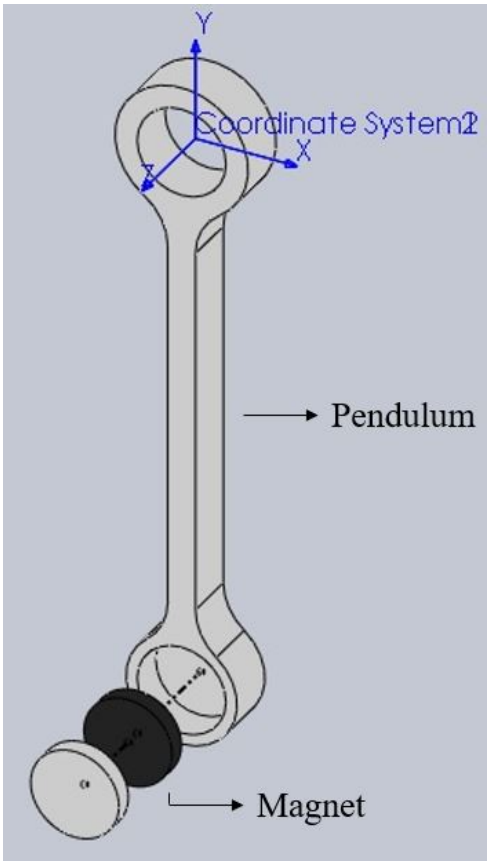

(a) Exploded view of the pendulum

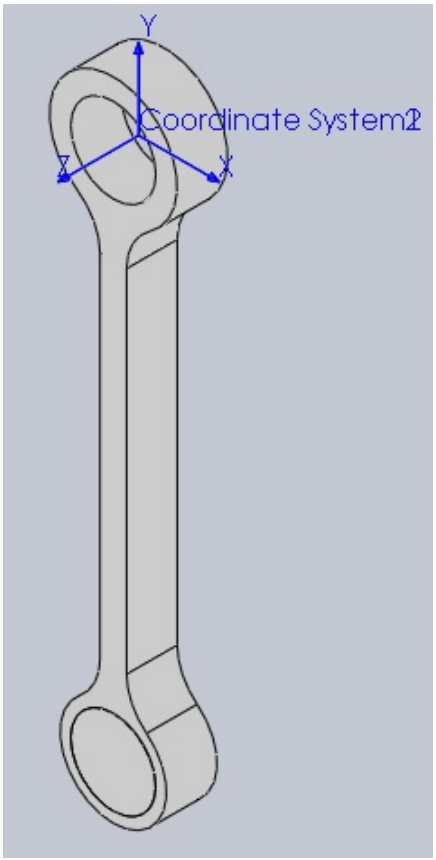

(b) Complete magnetic pendulum

Figure 3.3: Pendulum design in SolidWorks.

Recall that the length of the pendulum was chosen to be $l = 10$ cm. The design centre-to-centre distance between the pendulum magnets is $a = 37$ mm. Then, the bending moment at the suspension point, T_x, can be calculated using Eq. (3.11)

$$T_x = -0.0159 \ N.m \tag{3.13}$$

The width of the pendulum at the suspension point was designed to be $w = 24$ mm and the thickness which was chosen for the pendulum is $t = 9.525$ mm. Hence, with these quantities, the centroidal moment of inertia was determined using Eq. (3.2) to be

$$I = 5.761 \times 10^{-10} \ m^4 \tag{3.14}$$

Finally, the maximum stress, σ_{max}, can be derived by substituting Eqs. (3.13) and (3.14) into Eq. (3.1) and also considering $c = t/2 = 4.762$ mm.

$$\sigma_{max} = 0.131\ Mpa \tag{3.15}$$

The ultimate strength of PMMA is $\sigma_U = 70$ Mpa, So the maximum stress which is found, Eq. (3.15), is much lower than the ultimate strength and the pendulum is appropriately designed.

$$\sigma_{max} < \sigma_U \tag{3.16}$$

The magnet is attached to the pendulum by adhesive. To prevent magnets from detaching from the pendulums due to the magnetic forces, another ring of the same material (PMMA) was added in front of the magnet. The pendulum as designed in **SolidWorks** is shown in Fig. 3.3.

3.3 Suspension Rod Design

To select an appropriate suspension rod to attach the pendulums to, the maximum deflection of the rod was calculated assuming that it was loaded by the weight of eight equally spaced identical pendulum magnets. The maximum deflection of the suspension rod should have been less than 1 mm to be an acceptable design *i.e.* $\delta_{max} < 1$ mm.

Maximum deflection occurs at the middle of the rod and can be determined by the following equation [21].

$$\delta_{max} = -\frac{5qL^4}{384EI} \tag{3.17}$$

where q is the distributed load on the rod (force per unit length), L is the length of the rod, E is Young's modulus of elasticity and I is the area moment of inertia of the cross section. The rod is supported by two simple supports with a uniform distributed load caused by weight of the magnetic pendulums. The experimental setup for eight magnetic pendulums and the side view of the rod loaded by eight magnetic pendulums are shown in Figs. 3.4 and 3.5 respectively.

The distributed load, q, can be found by dividing the total weight applied on the rod, W_{total}, by the rod's total length, L_{total}.

$$q = \frac{W_{total}}{L_{total}} \tag{3.18}$$

Figure 3.4: Experimental Setup for eight magnetic pendulums.

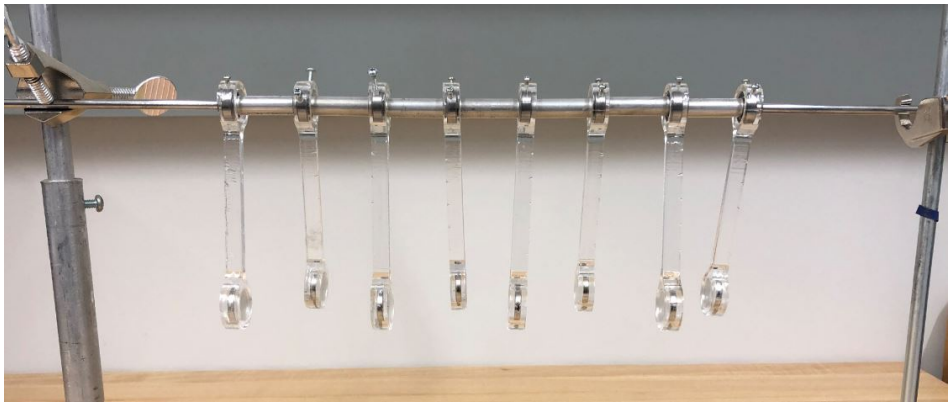

Figure 3.5: Side view of the rod loaded by eight magnetic pendulums.

The distance between the magnetic pendulums, a, and the distance between the first and last magnetic pendulums to the supports are considered to be 37 mm. The rod schematic diagram and the installation location of the magnetic pendulums are shown in Fig. 3.6. According to the figure, the total length of the rod is

$$L_{total} = 9 \times 37 = 333\ mm = 0.333\ m \tag{3.19}$$

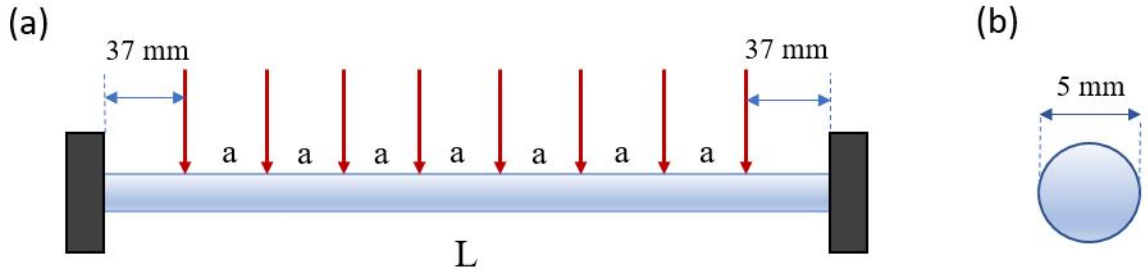

Figure 3.6: Schematic diagram of the rod: (a) Side view of the rod loaded by eight equally spaced magnetic pendulums, (b) Cross section of the rod.

The chosen magnet's mass is 4.71 g and the identified pendulum's mass is 10.07 g. Hence, the magnetic pendulum's mass will be 14.78 g. Moreover, the selected ball bearing had 0.57 g mass. Therefore, the total weight from the eight pendulums that the rod was loaded by is

$$W_{total} = M_{total} g = 1.204\ N \tag{3.20}$$

Thus, the distributed load is calculated using equations (3.19) and (3.20) in Eq. (3.18)

$$q = \frac{W_{total}}{L_{total}} = 3.62\ N/m \tag{3.21}$$

The area moment of inertia of the rod cross section can be derived using

$$I = \frac{\pi D_{dr}^4}{64} \tag{3.22}$$

where D_{dr} is the drill rod diameter. The 5 mm drill rod with a Young's modulus elasticity of $E = 193$ Gpa was chosen for the experiment setup. Hence, the area moment of inertia of the rod is $I = 30.68$ mm^4. The rod's parameter values are given in Table 3.4.

Table 3.4: Dimensions and parameter values for the drill rod.

Description	Symbol	Value [SI]
Drill rod diameter	D_{dr}	5 mm
Drill rod length	L	333 mm
Drill rod moment of inertia	$I = \frac{\pi D_{dr}^4}{64}$	30.68 mm^4
Drill rod Young's modulus	E	193 GPa

Ultimately, the maximum deflection, δ_{max}, can be derived by substituting Eqs. (3.19) and (3.21) into Eq. (3.17) to obtain

$$\delta_{max} = -\frac{5qL^4}{384EI} = -9.79 \times 10^{-5} m \tag{3.23}$$

The maximum deflection is approximately $\delta_{max} \simeq 0.098$ mm and it is smaller than 1 mm

$$\delta_{max} < 1mm \tag{3.24}$$

Hence, the suspension rod is properly selected.

Chapter 4

Results

In this chapter, the analytical response of the rigid body model is validated. In order to reach this goal, the equations of motions of the rigid body model were numerically solved and the nonlinear response of the system as well as the equilibrium points were compared with the experimental results. Furthermore, to have a better understanding of the magnetic pendulums interactions, a diagram of the simulated magnetic forces acting on first pendulum along with the response of the first and second pendulums are presented over time.

This chapter is organized as follows: Section 4.1 describes a numerical solution of the rigid body model equations of motions. In section 4.2, the model parameters are experimentally identified and the nonlinear response of the system is analyzed in section 4.3. Then, the equilibrium points and the magnetic forces diagram are investigated.

4.1 Numerical Solution

To determine the response of the rigid body system, the equations of motions derived in Section 2.6 are numerically solved. For the first pendulum and for the case of $J_1 \neq J_2$ and $c_1 \neq c_2$, recall that Eq. (2.125) can be written as

$$\ddot{\theta}_1 + \left(\frac{c_1}{J_{zz1}}\right)\dot{\theta}_1 - \left(\frac{F_{y1}l}{J_{zz1}} - \frac{mgd}{J_{zz1}}\right)\sin\theta_1 - \left(\frac{F_{x1}l}{J_{zz1}}\right)\cos\theta_1 = 0 \tag{4.1}$$

where m is the rigid body mass, d is the distance between the point of suspension and the center of mass and g is acceleration of gravity. The magnetic interaction forces F_{x1} and

F_{y1} are obtained from Eq. (2.120). We introduce the change of variables

$$x_1 = \theta_1 \tag{4.2}$$
$$x_2 = \dot{\theta}_1 \tag{4.3}$$

to recast the equation in state-space form, which yields

$$\dot{x}_1 = x_2 \tag{4.4}$$
$$\dot{x}_2 = -\left(\frac{c_1}{J_{zz1}}\right) x_2 + \left(\frac{F_{y1}l}{J_{zz1}} - \frac{mgd}{J_{zz1}}\right) \sin x_1 + \left(\frac{F_{x1}l}{J_{zz1}}\right) \cos x_1 \tag{4.5}$$

For the second pendulum, recall from Eq. (2.131)

$$\ddot{\theta}_2 + \left(\frac{c_2}{J_{zz2}}\right) \dot{\theta}_2 - \left(\frac{F_{y2}l}{J_{zz2}} - \frac{mgd}{J_{zz2}}\right) \sin \theta_2 - \left(\frac{F_{x2}l}{J_{zz2}}\right) \cos \theta_2 = 0 \tag{4.6}$$

where the magnetic interaction forces F_{x2} and F_{y2} are obtained from Eq. (2.127). Again, we use the change of variables

$$x_3 = \theta_2 \tag{4.7}$$
$$x_4 = \dot{\theta}_2 \tag{4.8}$$

to recast the equation in state-space form, which yields

$$\dot{x}_3 = x_4 \tag{4.9}$$
$$\dot{x}_4 = -\left(\frac{c_2}{J_{zz2}}\right) x_4 + \left(\frac{F_{y2}l}{J_{zz2}} - \frac{mgd}{J_{zz2}}\right) \sin x_3 + \left(\frac{F_{x2}l}{J_{zz2}}\right) \cos x_3 \tag{4.10}$$

Eqs. (4.4), (4.5), (4.9) and (4.10) were numerically solved in **MATLAB** using the *ode45* solver. The relative tolerance and absolute tolerance were both set to 10^{-6}. The identified dimensions and parameter values used in the numerical solution are given in Table 4.1.

4.2 Parameter Identification

To estimate the damping coefficient c, a simple experiment was performed with only one pendulum. The pendulum was released from 90 degrees and allowed to oscillate freely. The

Table 4.1: Identified dimensions and parameter values for the numerical solution.

Property	Symbol	Value
Pendulum mass	m	14.78×10^{-3} kg
Pendulum length	l	0.1 m
Gravitational acceleration	g	9.804 m/s^2
First pendulum's damping coefficient	c_1	2.239×10^{-5} kg.m^2.s^{-1}
Second pendulum's damping coefficient	c_2	4.596×10^{-5} kg.m^2.s^{-1}
Pendulum magnet separation	a	41.07×10^{-3} m
Permeability of free space	μ_0	$4\pi \times 10^{-7}$ H·m^{-1}
DA2-N52 magnet volume	V	0.628×10^{-6} m^3
DA2-N52 magnet residual flux density	B_r	1.273 Tesla
Pendulum mass moment of inertia	J_{zz}	886.763×10^{-7} kg.m^2
Distance from center of gravity to origin	d	0.0656 m

amplitude of oscillations was measured over four periods and the logarithmic decrement was calculated using the following formula

$$\delta = \frac{1}{(n-1)} ln \frac{X_1}{X_n} \tag{4.11}$$

where X_n is the displacement at the nth peak. Then, the damping ratio, ζ, can be calculated by solving for it in the equation

$$\delta = \frac{2\pi\zeta}{\sqrt{1-\zeta^2}} \tag{4.12}$$

Ultimately, recalling Eq. (4.1) or Eq. (4.6), the damping coefficient can be found as

$$c = 2\zeta J_{zz} \omega_n \tag{4.13}$$

where ω_n is the natural frequency of the system.

To find ω_n, first the period of damped oscillations was measured, τ_d, and used to calculate the damped natural frequency of the pendulum as

$$\omega_d = \frac{2\pi}{\tau_d} \tag{4.14}$$

Table 4.2: Measured amplitudes over four periods.

X_1	X_2	X_3	X_4	X_5
84.035°	69.813°	57.459°	46.969°	38.369°

The natural frequency of the pendulum can then be found from the equation

$$\omega_n = \frac{\omega_d}{\sqrt{1-\zeta^2}} \tag{4.15}$$

Similarly, from Eq. (4.1) or Eq. (4.6), J_{zz} can be written as

$$J_{zz} = \frac{mgd}{\omega_n^2} \tag{4.16}$$

Finally, by substituting Eqs. (4.14), (4.15) and (4.16) into Eq. (4.13), the damping coefficient is obtained.

The oscillation amplitudes were measured over four periods as listed in Table 4.2. The logarithmic decrement was calculated from Eq. (4.11) as

$$\delta = 0.196 \tag{4.17}$$

and the damping ratio is found from Eq. (4.12) to be

$$\zeta = 0.031 \tag{4.18}$$

The period of damped oscillations was measured as $\tau_d = 0.60$ s. Thus, from Eq. (4.14), the damped natural frequency is

$$\omega_d = 10.472\ rad/s = 1.66\ Hz \tag{4.19}$$

and from Eq. (4.15)

$$\omega_n = 10.477\ rad/s = 1.67\ Hz \tag{4.20}$$

By substituting the values of m, g and d from Table 4.1 and the obtained natural frequency in Eq. (4.16), the mass moment of inertia about Z axis is

$$J_{zz} = 865.98 \times 10^{-7}\ kg.m^2 \tag{4.21}$$

for both the first and second pendulums. Ultimately, from Eq. (4.13) the damping coefficient is

$$c = 5.625 \times 10^{-5}\ kg.m^2.s^{-1} \tag{4.22}$$

It is worthwhile to note that c_1 and c_2 are not equal because of differences in the bearings and installation of the individual pendulums.

4.3 Time-History Analysis

The design dimensions and identified parameters listed in Table 4.1 were used to simulate the response of the first and second pendulums to the initial conditions:

$$\begin{aligned} \theta_1(0) &= 90^\circ \quad , \quad \dot{\theta}_1(0) = 0 \\ \theta_2(0) &= 0 \quad , \quad \dot{\theta}_2(0) = 0 \end{aligned} \tag{4.23}$$

The simulated and experimentally measured angular displacements of the first and second pendulums are shown in Figs. 4.1 and 4.2 respectively.

The simulation and experiment responses are in good agreement as it is displayed in the figures 4.1 and 4.2. Two stages can be observed in the pendulums' oscillations. In the first stage following the first pendulum release, its oscillations resemble those of a simple (single) pendulum for the first seven periods seconds due to the dominance of gravitational potential energy over the magnetic potential energy. Meanwhile, the second pendulum gains kinetic energy from the first pendulum and starts to oscillate due to the magnetic interaction. During this stage, the first pendulum oscillations diminish while those of the second pendulum grow. In the second stage, magnetic potential energy dominates gravitational potential energy and a second harmonic appears in the oscillations of the first and second pendulums.

Fast Fourier Transform (FFT) of the first and second pendulums simulated and measured responses are shown in Fig. 4.3. As illustrated, the experimental natural frequency of the first pendulum is 1.524 Hz and the simulated natural frequency is relatively close at 1.5 Hz with a difference of 1.6%. The experimental natural frequency of the second pendulum is 1.515 Hz and the simulated natural frequency is 1.5 Hz with a difference of $\approx$ 1%. This frequency corresponds to the dominant harmonic in the first stage of the pendulums' oscillations.

As it is shown in Fig. 4.3, the average amplitude of the first pendulum is more than the average amplitude of the second pendulum due to the fact that the first pendulum was released from 90 degrees with a significant amount of potential energy but the second pendulum started oscillation from rest at its equilibrium point and gained kinetic energy from the first pendulum via magnetic interaction only. It can also be observed that the simulation peak points for both pendulums are smaller than the experimental peak points particularly for the second pendulum peak.

The simulated free response of the pendulums for initial conditions identical to those of Eq. (4.23) except that $\theta_1(0)$ is varied from 90° to 20° are displayed in Fig. 4.4. As can be

seen from the figure, when the first pendulum is released from an angle of 40° or lower, the pendulums do not cross each other, $\theta_1 = \theta_2$, with each pendulum oscillating primarily on the either side of the vertical plane (X-Y) where it was located before oscillations started. This is due to the fact that the first pendulum's potential energy in those cases is not enough to overcome the repulsive magnetic force among the magnets required to pass the adjacent pendulum.

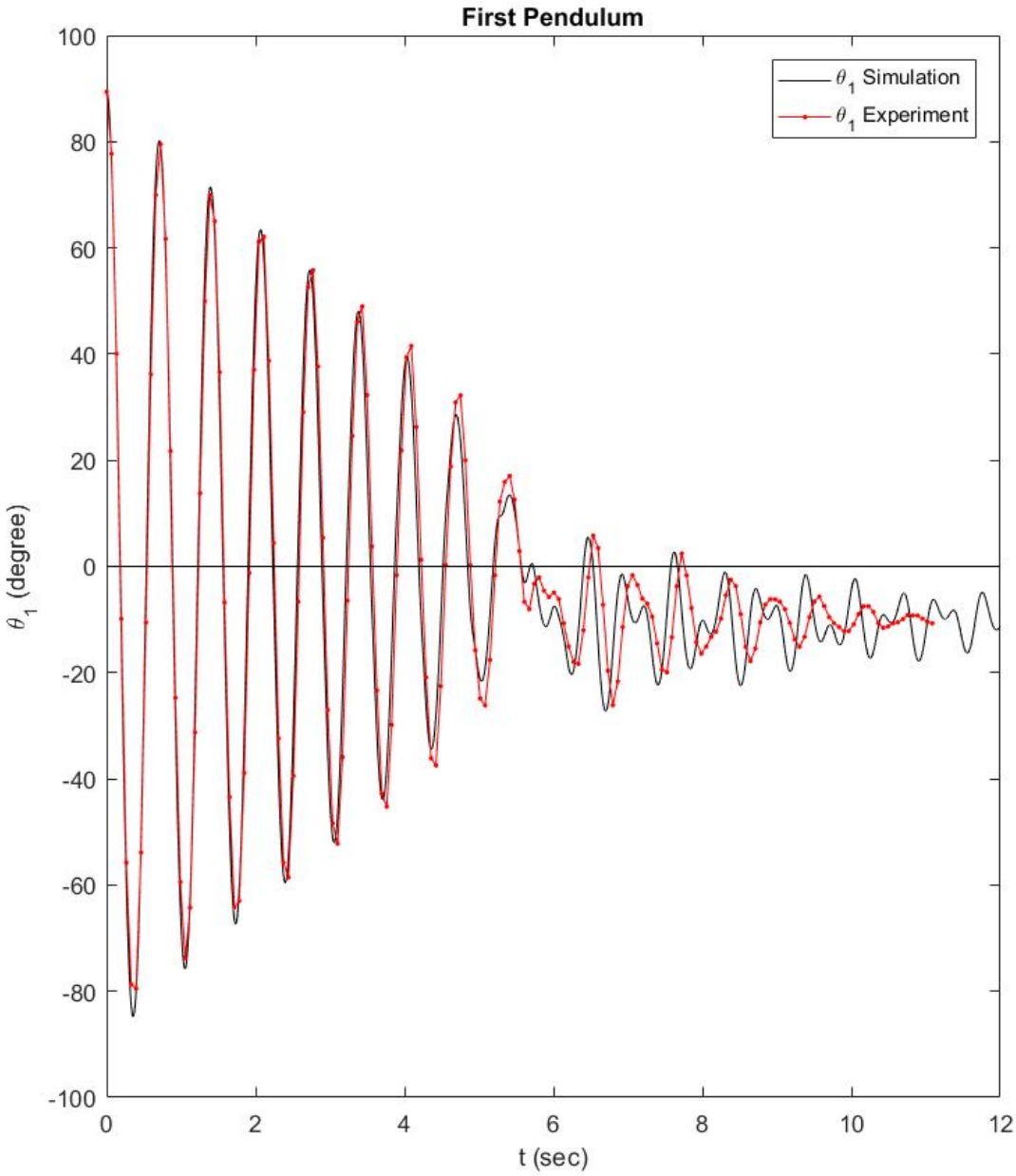

Figure 4.1: The simulated (black line) and measured (red dotted line) angular displacement $\theta_1(t)$ of the first pendulum as functions of time.

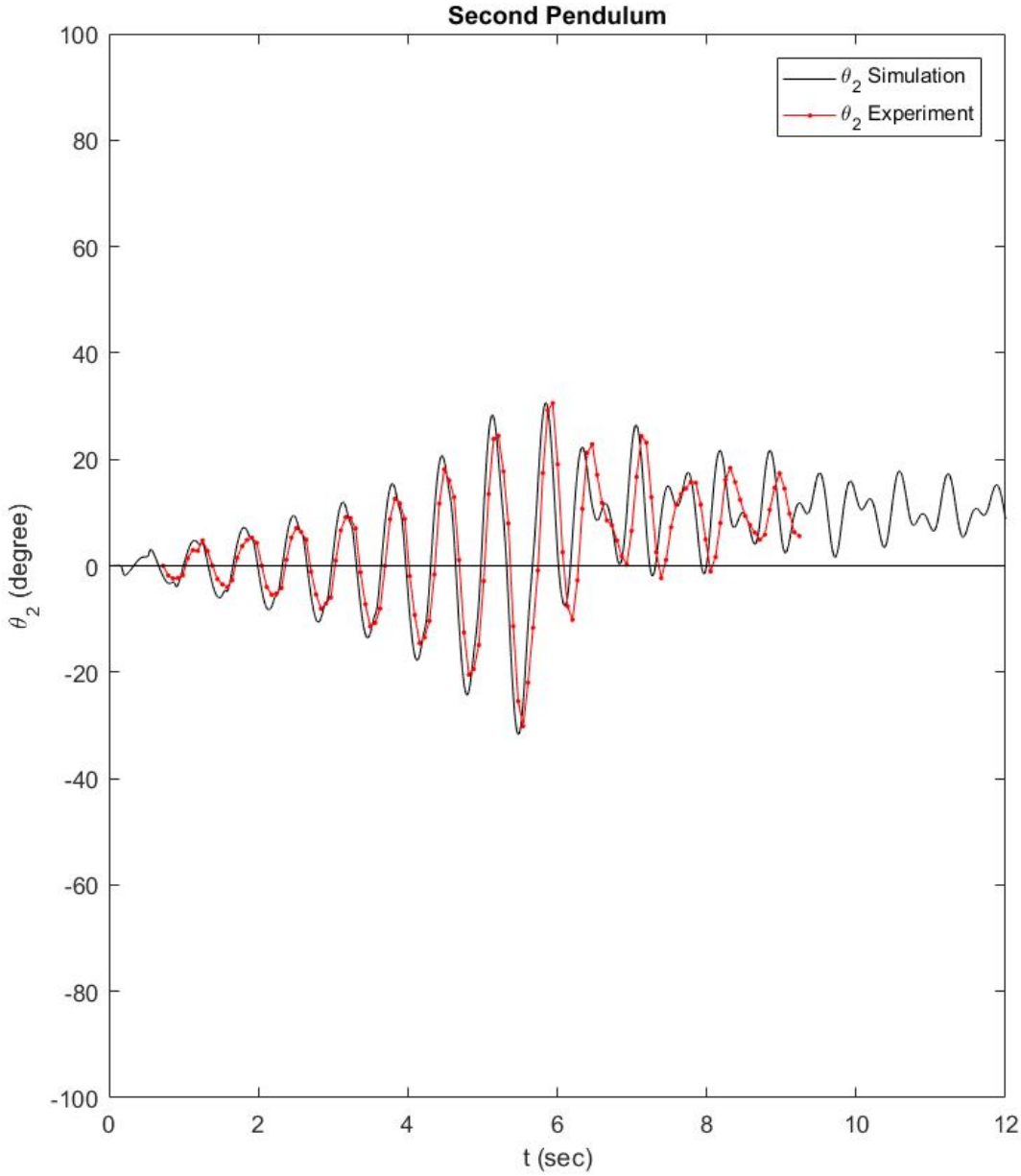

Figure 4.2: The simulated (black line) and measured (red dotted line) angular displacement $\theta_2(t)$ of the second pendulum as functions of time.

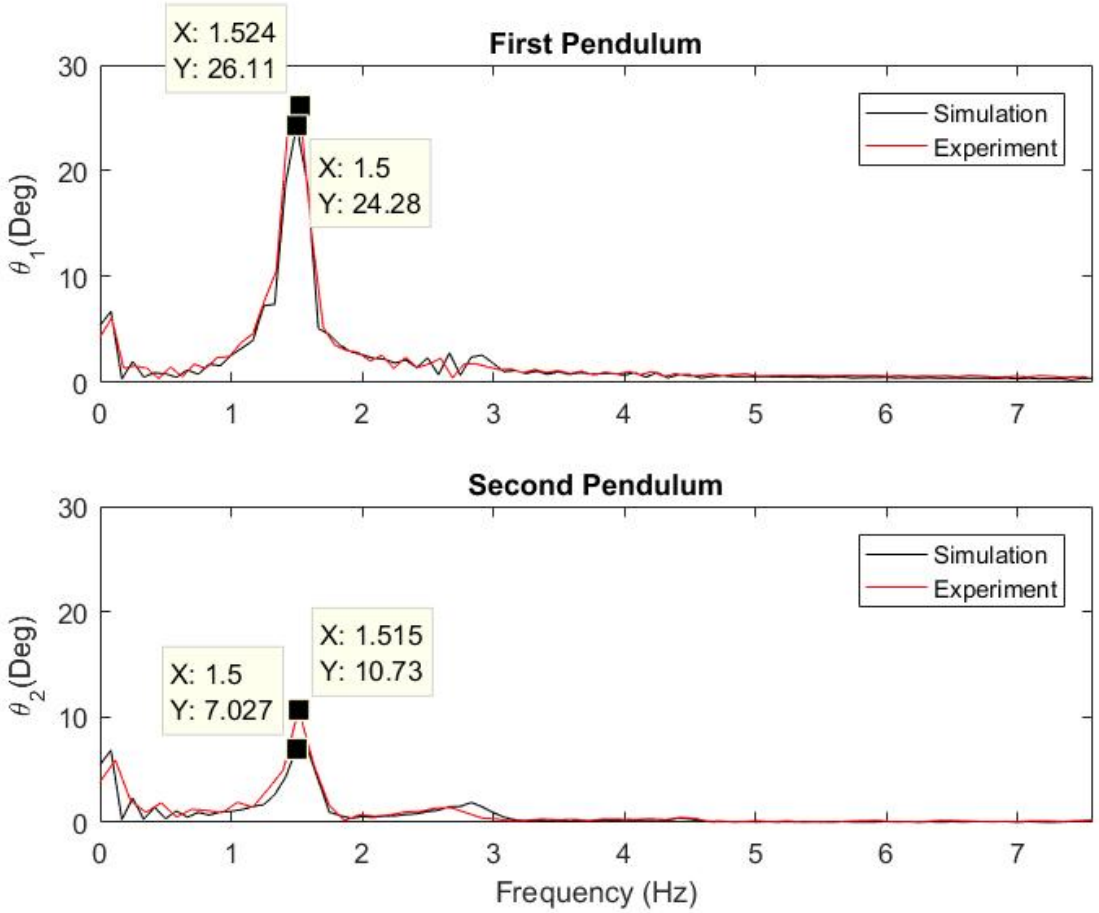

Figure 4.3: Fast Fourier Transform (FFT) for the first and second pendulums' angular displacements.

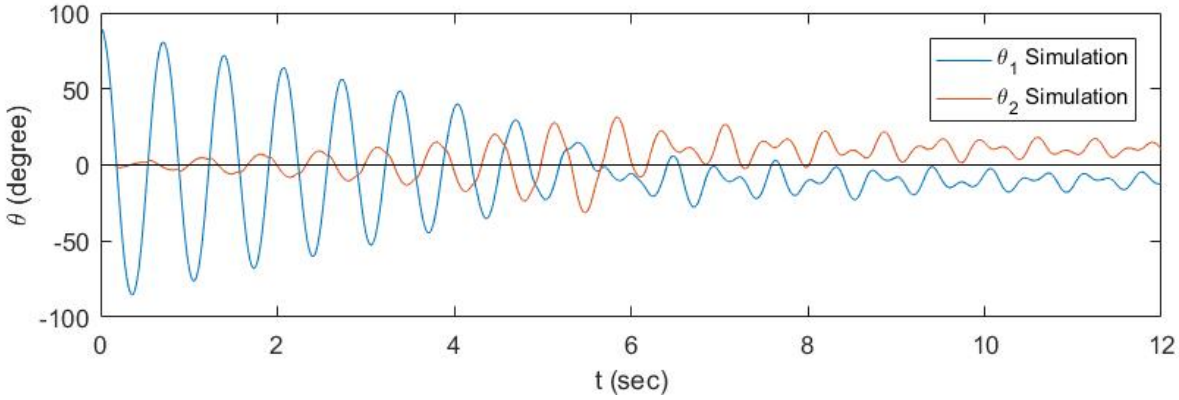

(a) $\theta_1(0) = 90°$

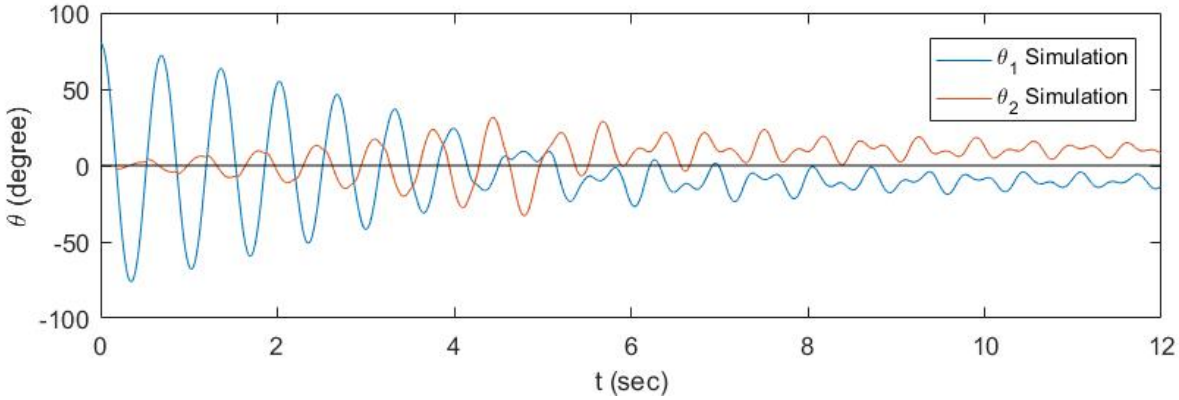

(b) $\theta_1(0) = 80°$

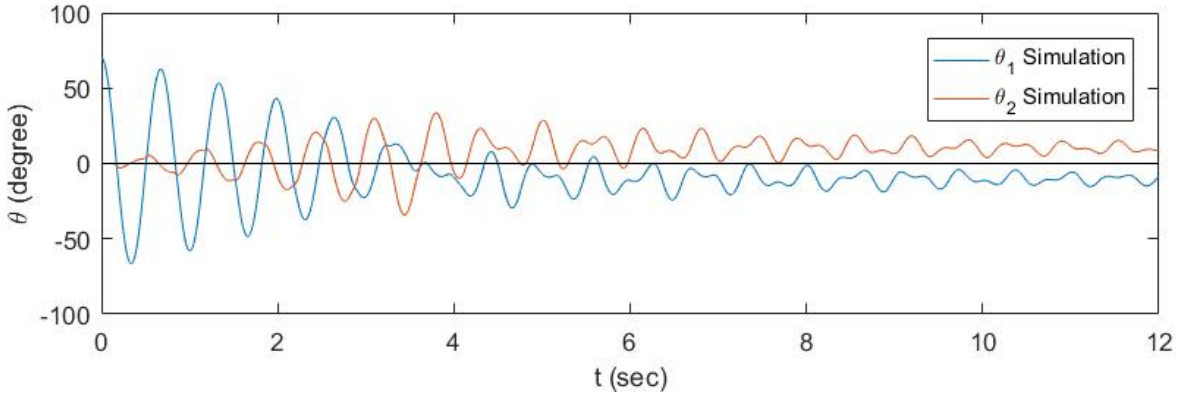

(c) $\theta_1(0) = 70°$

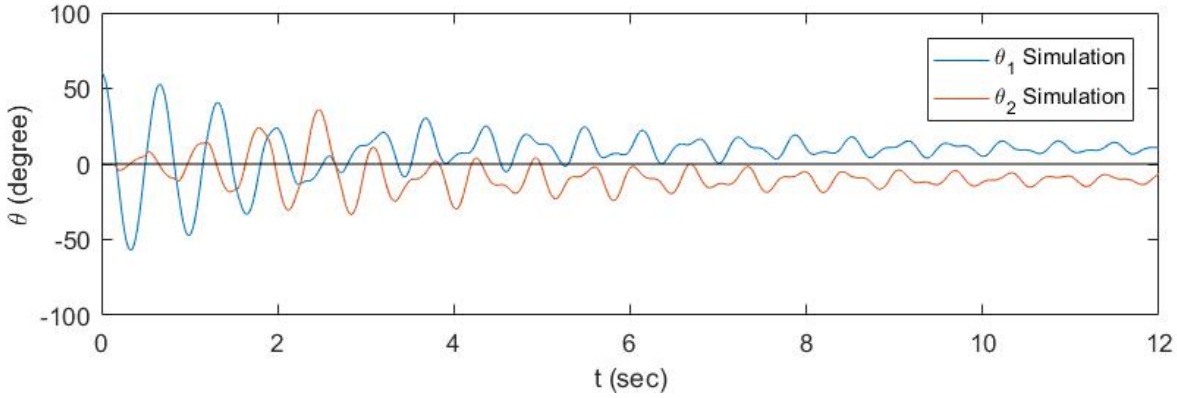

(d) $\theta_1(0) = 60°$

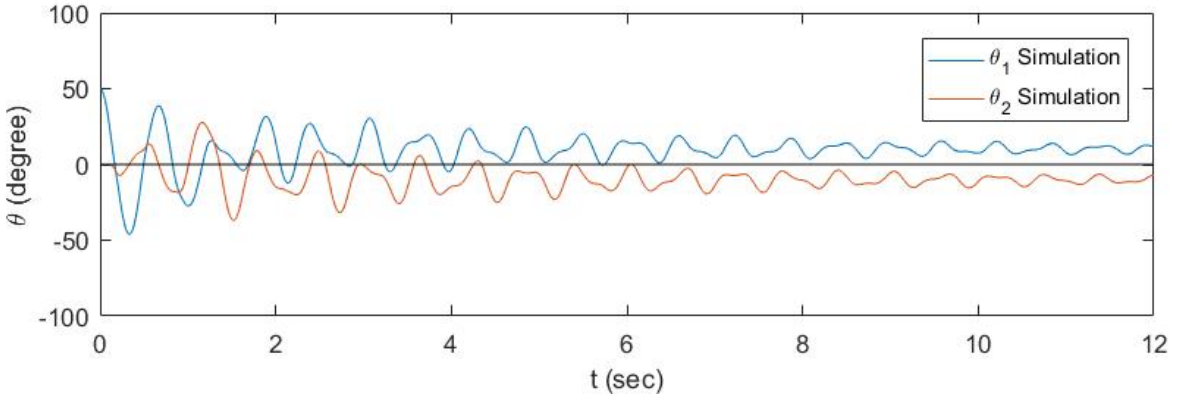

(e) $\theta_1(0) = 50°$

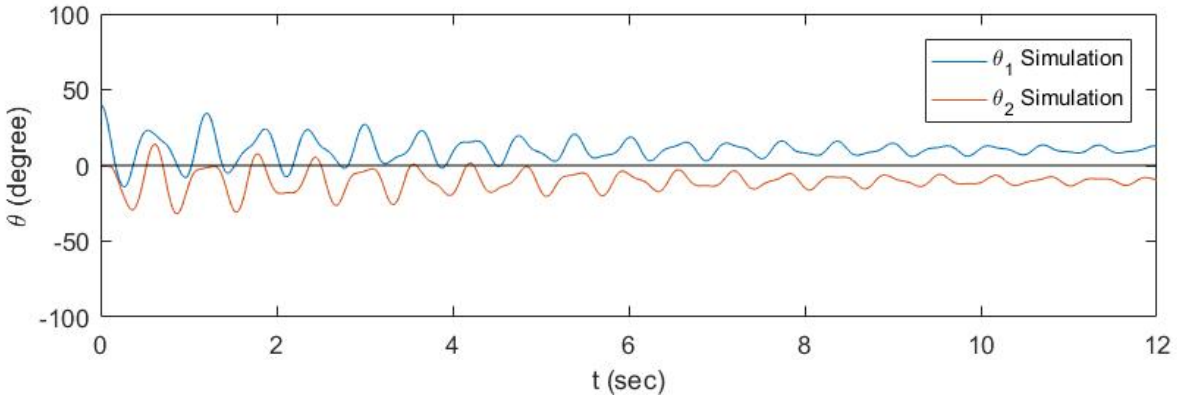

(f) $\theta_1(0) = 40°$

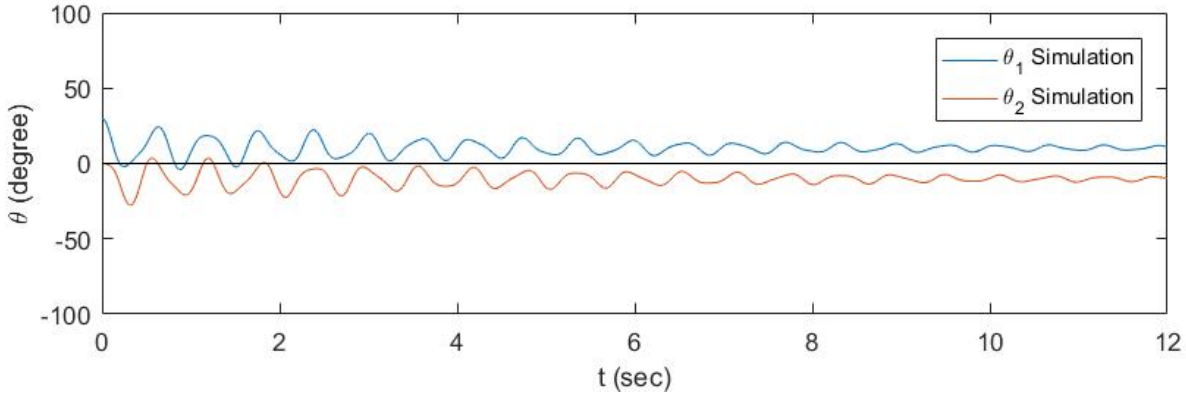

(g) $\theta_1(0) = 30°$

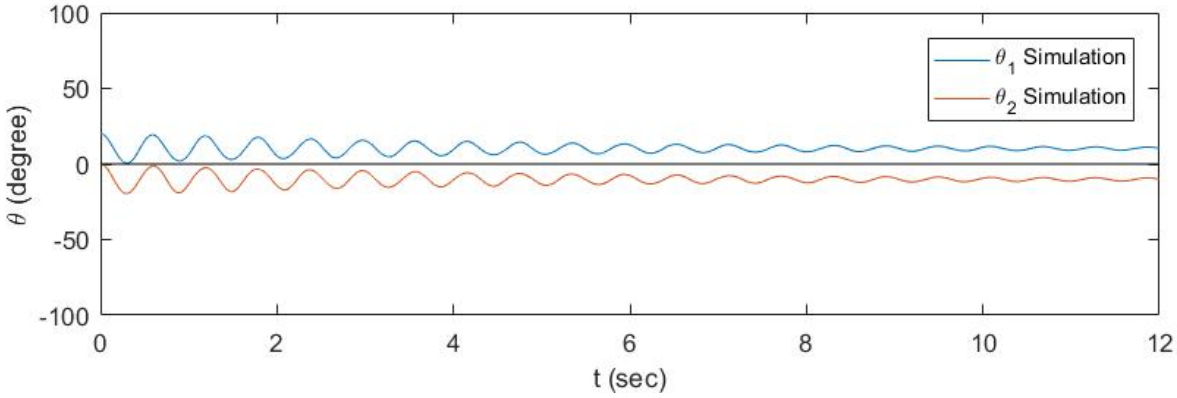

(h) $\theta_1(0) = 20°$

Figure 4.4: Pendulums responses for different initial conditions.

4.4 Equilibrium Points

Evaluating the system equilibrium points is a fundamental step to determine its stability. To determine the equilibrium points of the two-pendulum system, we set the time derivatives $\dot{\theta}_1, \dot{\theta}_2, \ddot{\theta}_1$ and $\ddot{\theta}_2$ equal to zero in Eqs. (4.1) and (4.6) to obtain:

$$\left(\frac{F_{y1}l}{J_{zz}} - \frac{mgd}{J_{zz}}\right)\sin\theta_1 + \left(\frac{F_{x1}l}{J_{zz}}\right)\cos\theta_1 = 0 \tag{4.24}$$

$$\left(\frac{F_{y2}l}{J_{zz}} - \frac{mgd}{J_{zz}}\right)\sin\theta_2 + \left(\frac{F_{x2}l}{J_{zz}}\right)\cos\theta_2 = 0 \tag{4.25}$$

We solve these algebraic equations simultaneously to find the equilibrium points (θ_1, θ_2).

Table 4.3: Equilibrium points and their stability.

Equilibrium Points (θ_1, θ_2)	Stability	Reason
$(0, 0)$	Unstable	Magnetic Force
$(0, 180)$	Unstable	Gravitational Force
$(180, 0)$	Unstable	Gravitational Force
$(180, 180)$	Unstable	Magnetic Force and Gravitational Force
$(-10.2018, 10.2018)$	Stable	Magnetic Force
$(10.2018, -10.2018)$	Stable	Magnetic Force

By solving the Eqs. (4.24) and (4.25) simultaneously in **MATLAB** using *fsolve*, the six equilibrium points listed in Table 4.3 are obtained. The first equilibrium point is $(0, 0)$ which is unstable due to the magnetic force of the rebelling magnets. The two magnets strongly repel each other and move the pendulums away from this equilibrium upon any small perturbation of either pendulum away from this equilibrium point. In contrast, this equilibrium point is stable for two attractive magnets.

Two more unstable equilibrium points, $(0, 180)$ and $(180, 0)$, are symmetrical with respect to the horizontal plane (X-Z). The instability of these points is because of the gravitational force. Another unstable equilibrium point is $(180, 180)$ where the instability is due to the magnetic force as well as the gravitational force.

The fifth equilibrium point

$$(\theta_1, \theta_2) = (-10.2018^\circ, +10.2018^\circ) \tag{4.26}$$

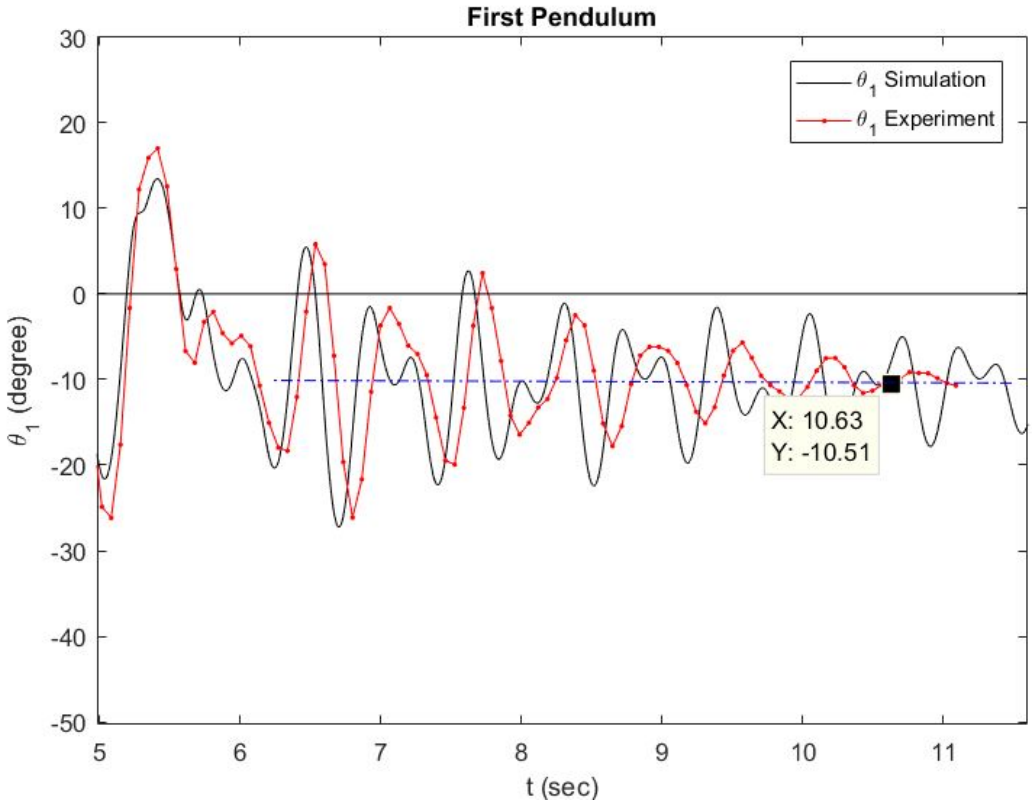

Figure 4.5: The equilibrium point of the first pendulum measured experimentally.

is stable. It describes equilibrium positions for the first and second pendulums that are symmetrical with respect to the vertical plane. In comparison, the equilibrium point measured experimentally and shown in Figs. 4.5 and 4.6, is

$$(\theta_1, \theta_2) = (-10.51^\circ, +10.53^\circ) \tag{4.27}$$

which is quite close to that obtained from the model. The last stable equilibrium point $(10.2018, -10.2018)$ is also symmetrical with respect to the vertical plane. It was also observed experimentally.

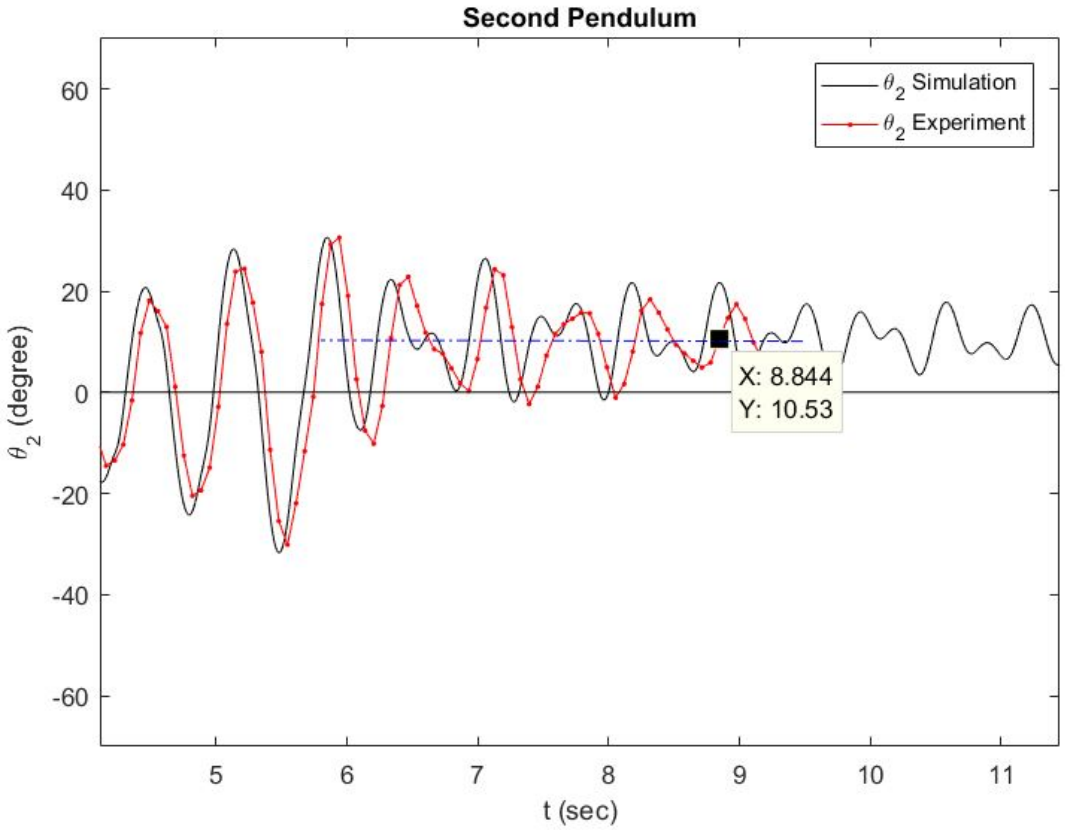

Figure 4.6: The equilibrium point of the second pendulum measured experimentally.

4.5 Magnetic Forces

To have a better understanding of a magnetic pendulum interactions, variation of the magnetic forces over time is investigated. The magnetic force acting on the first pendulum, for the special case of two identical pendulums where the magnets are arranged to obtain a repulsive interaction force, are computed in Eq. (2.36). By substituting Eqs. (2.37) and (2.38) in Eq. (2.36), the magnetic force acting upon the first pendulum can be rewritten as:

$$F_{x1} = \frac{3\mu_0\mu^2}{4\pi}\left[\frac{5a^2l(\sin\theta_1 - \sin\theta_2)}{(a^2+2l^2(1-\cos(\theta_2-\theta_1)))^{7/2}} - \frac{l(\sin\theta_1 - \sin\theta_2)}{(a^2+2l^2(1-\cos(\theta_2-\theta_1)))^{5/2}}\right] \tag{4.28}$$

$$F_{y1} = \frac{3\mu_0\mu^2}{4\pi}\left[\frac{-5a^2l(\cos\theta_1 - \cos\theta_2)}{(a^2+2l^2(1-\cos(\theta_2-\theta_1)))^{7/2}} + \frac{l(\cos\theta_1 - \cos\theta_2)}{(a^2+2l^2(1-\cos(\theta_2-\theta_1)))^{5/2}}\right] \tag{4.29}$$

$$F_{z1} = \frac{3\mu_0\mu^2}{4\pi}\left[\frac{-5a^3}{(a^2+2l^2(1-\cos(\theta_2-\theta_1)))^{7/2}} + \frac{3a}{(a^2+2l^2(1-\cos(\theta_2-\theta_1)))^{5/2}}\right] \tag{4.30}$$

The simulated response of the first and second pendulums over time along with the magnetic force acting on the first pendulum are shown in Fig. 4.7. Up to 5.6 seconds, the pendulums are crossing each other as indicated by the constant peak values of F_x and F_z corresponding to the constant minimum distance a between the magnets when they cross each other. Henceforth, the peak values of F_x and F_z decrease monotonically as the pendulums cease to cross each other and the minimum distance-per-period increases, and eventually approach $F_x = -0.0171$ N and $F_z = 0.0014$ N at the equilibrium point.

The magnitude of F_y approaches zero as the pendulums approach their equilibrium positions. This is due to the fact that at the equilibrium point the magnets are at the same height. Hence, the magnetic force has no y component and $F_y = 0$.

A more detailed study of the magnetic force during pendulums crossing is given in Fig. 4.8. When the two magnets cross, their angular position is identical, $\theta_1 = \theta_2$. By substituting $\theta_1 = \theta_2$ in Eqs. (4.28) to (4.30), we find that $F_x = 0$, $F_y = 0$ and F_z is maximum. These results are in agreement with the simulation results shown in Fig. 4.8. Furthermore, it can be observed from Fig. 4.8 that before the two magnets cross each other, F_x and F_y are at maxima and after crossing they are again at maxima but in opposite direction.

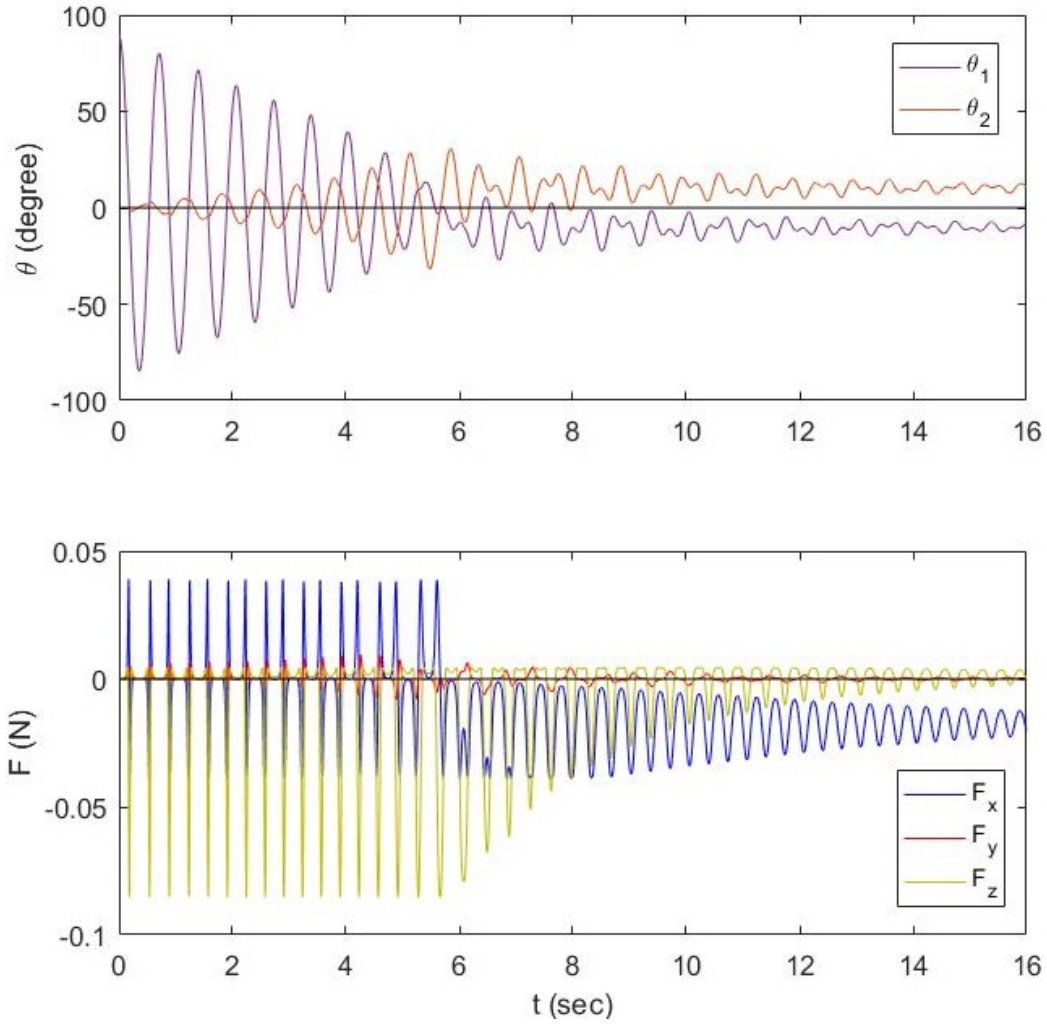

Figure 4.7: The simulation response of the first and second pendulums and the diagram of the magnetic forces on the first pendulum over time.

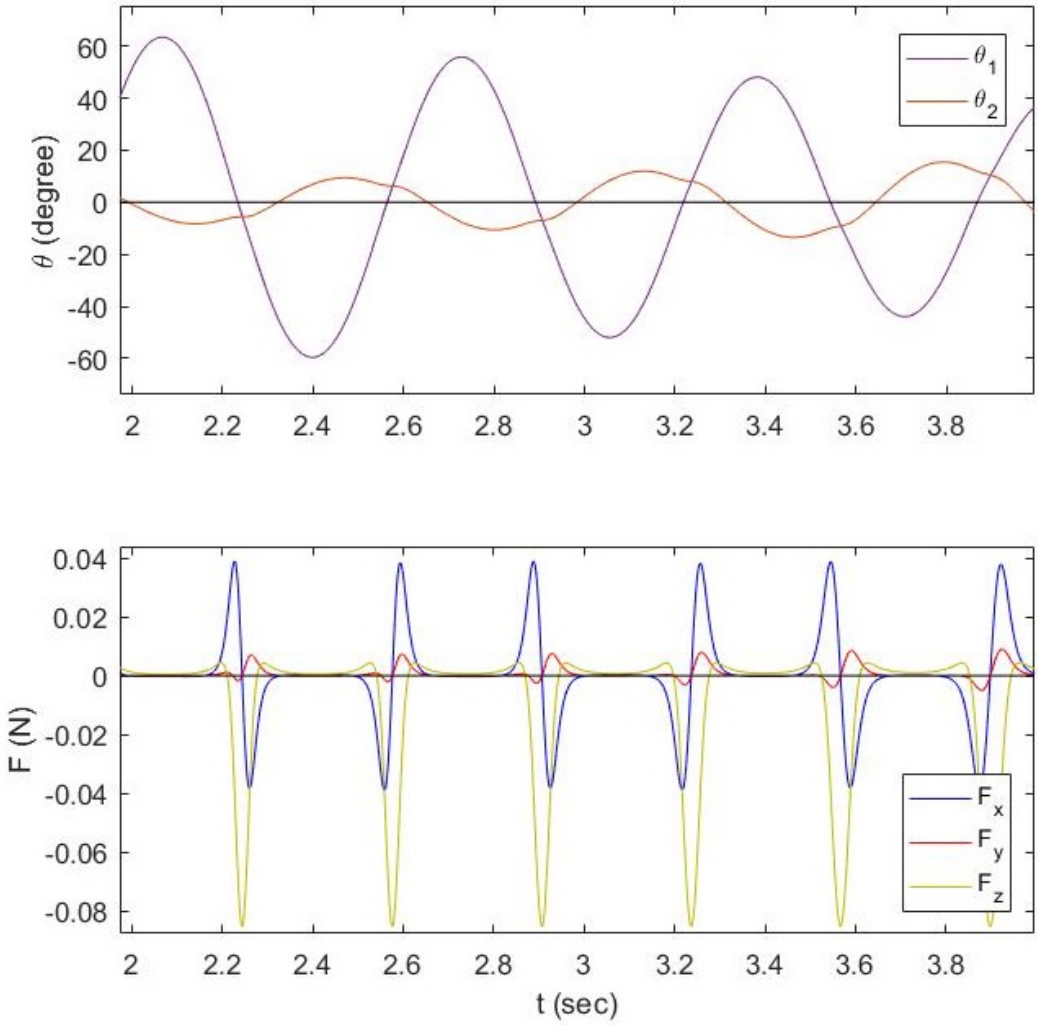

Figure 4.8: More details of magnets crossing points and the relevant magnetic forces on the first pendulum.

Chapter 5

Conclusion and Future Work

A fundamental field that coupled nonlinear oscillators and specifically coupled magnetic oscillators may play a crucial role in is atomic physics. Due to the qualitative similarity of the magnetic field and the electromagnetic field governing the atoms in the lattice structure in crystalline solids, investigating the coupled magnetic oscillators could help researchers to have a better understanding of atoms in a lattice behaviour.

In this thesis a model of a chain of two dimensional magnetic pendulums using an ideal point mass model and a rigid body model has been derived. The nonlinear dynamics of the models through finding the interaction forces between the magnets has been investigated. With the aim of demonstrating the dynamics of the system completely, the equations of motion of the pendulum magnets have been analytically derived and by linearizing the equations of motion, the natural frequencies of the system have been found.

The behaviour of the simulated system has been examined experimentally to ensure the accuracy of the analytical approach. To achieve this, a simple experimental setup consisting of two coupled magnetic pendulums has been designed. The equations of motions of a rigid body model including the determined magnetic forces have been numerically solved and the nonlinear response of the system along with the equilibrium points and the system's frequency have been validated experimentally. As it has been described in Section 4.3, the simulation and experiment results have been in good agreement.

The recommended future work for expanding this research is to replace the magnetic point source magnet model with a three dimensional magnet model. A further extension to this work would be to experimentally and analytically investigate a series of more than two pendulums.

References

[1] CB Williams and Rob B Yates. Analysis of a micro-electric generator for microsystems. *Sensors and Actuators A: Physical*, 52(1–3):8–11, 1996.

[2] Joseph A Paradiso and Thad Starner. Energy scavenging for mobile and wireless electronics. *IEEE Pervasive computing*, (1):18–27, 2005.

[3] D Dane Quinn, Angela L Triplett, Lawrence A Bergman, and Alexander F Vakakis. Comparing linear and essentially nonlinear vibration-based energy harvesting. *Journal of Vibration and Acoustics*, 133(1):011001, 2011.

[4] Somayyeh Belbasi, M Ebrahim Foulaadvand, and Yong S Joe. Anti-resonance in a one-dimensional chain of driven coupled oscillators. *American Journal of Physics*, 82(1):32–38, 2014.

[5] R Jothimurugan, K Thamilmaran, S Rajasekar, and MAF Sanjuán. Multiple resonance and anti-resonance in coupled duffing oscillators. *Nonlinear Dynamics*, 83(4):1803–1814, 2016.

[6] OV Gendelman, DV Gorlov, LI Manevitch, and AI Musienko. Dynamics of coupled linear and essentially nonlinear oscillators with substantially different masses. *Journal of Sound and Vibration*, 286(1-2):1–19, 2005.

[7] Diala Bitar, Najib Kacem, and Noureddine Bouhaddi. Investigation of modal interactions and their effects on the nonlinear dynamics of a periodic coupled pendulums chain. *International Journal of Mechanical Sciences*, 127:130–141, 2017.

[8] A Jallouli, N Kacem, and N Bouhaddi. Stabilization of solitons in coupled nonlinear pendulums with simultaneous external and parametric excitations. *Communications in Nonlinear Science and Numerical Simulation*, 42:1–11, 2017.

[9] Miguel Molerón, Andrea Leonard, and Chiara Daraio. Solitary waves in a chain of repelling magnets. *Journal of Applied Physics*, 115(18):184901, 2014.

[10] Wei Wang, Junyi Cao, Dhiman Mallick, Saibal Roy, and Jing Lin. Comparison of harmonic balance and multi-scale method in characterizing the response of monostable energy harvesters. *Mechanical Systems and Signal Processing*, 108:252–261, 2018.

[11] Grzegorz Litak, Michael I Friswell, Cedrick A Kitio Kwuimy, Sondipon Adhikari, and Marek Borowiec. Energy harvesting by two magnetopiezoelastic oscillators with mistuning. *Theoretical and Applied Mechanics Letters*, 2(4):043009, 2012.

[12] Lihua Tang and Yaowen Yang. A nonlinear piezoelectric energy harvester with magnetic oscillator. *Applied Physics Letters*, 101(9):094102, 2012.

[13] PV Malaji and SF Ali. Magneto-mechanically coupled electromagnetic harvesters for broadband energy harvesting. *Applied Physics Letters*, 111(8):083901, 2017.

[14] Jae Yong Cho, Sinwoo Jeong, Hamid Jabbar, Yewon Song, Jung Hwan Ahn, Jeong Hun Kim, Hyun Jun Jung, Hong Hee Yoo, and Tae Hyun Sung. Piezoelectric energy harvesting system with magnetic pendulum movement for self-powered safety sensor of trains. *Sensors and Actuators A: Physical*, 250:210–218, 2016.

[15] FM Russell, Y Zolotaryuk, JC Eilbeck, and T Dauxois. Moving breathers in a chain of magnetic pendulums. *Physical Review B*, 55(10):6304, 1997.

[16] Ahmed Mehrem, Noe Jimenez, LJ Salmerón-Contreras, X García-Andrés, LM García-Raffi, R Picó, and Víctor José Sánchez-Morcillo. Nonlinear dispersive waves in repulsive lattices. *Physical Review E*, 96(1):012208, 2017.

[17] Samuel C Stanton, Clark C McGehee, and Brian P Mann. Nonlinear dynamics for broadband energy harvesting: Investigation of a bistable piezoelectric inertial generator. *Physica D: Nonlinear Phenomena*, 239(10):640–653, 2010.

[18] K & J Magnetics Ltd. https://www.kjmagnetics.com/proddetail.asp?prod=DA2-N52. Accessed: 2019-04-16.

[19] KBC Tools Ltd. https://www.kbctools.ca/itemdetail?auto=1&itemcode=1-950M-005. Accessed: 2019-04-16.

[20] Bearings Canada Ltd. https://www.bearingscanada.com/625-Z-Radial-Ball-Bearing-Double-Shielded-Bore-p/625-z-bore-dia-5mm-od-16mm-5mm.htm. Accessed: 2019-04-16.

[21] Ferdinand P. Beer, Jr. E. Russell Johnston, John T. Dewolf, and David F. Mazurek. *Mechanics of Materials*. McGraw-Hill, 2012.

[22] Kar W Yung, Peter B Landecker, and Daniel D Villani. An analytic solution for the force between two magnetic dipoles. *Physical Separation in Science and Engineering*, 9(1):39–52, 1998.

APPENDICES

Appendix A

Force acting on magnetic dipole i due to magnetic dipole j

From Yung et al. [22] the force acting on magnetic dipole i due to magnetic dipole j is

$$\vec{F}_{mi} = \frac{3\mu_0}{4\pi r_{ij}^5}\left[(\vec{r}_{ij}\times\vec{\mu}_i)\times\vec{\mu}_j + (\vec{r}_{ij}\times\vec{\mu}_j)\times\vec{\mu}_i - 2(\vec{\mu}_i\cdot\vec{\mu}_j)\vec{r}_{ij} + \frac{5}{r_{ij}^2}(\vec{r}_{ij}\times\vec{\mu}_i)\cdot(\vec{r}_{ij}\times\vec{\mu}_j)\vec{r}_{ij}\right] \tag{A.1}$$

where $\vec{r}_{ij}$ is the position of magnet i with respect to magnet j (or equivalently the vector from magnet j to magnet i) such that

$$\vec{r}_{ij} = \vec{r}_i - \vec{r}_j \tag{A.2}$$

and the magnitude of $\vec{r}_{ij}$ is

$$r_{ij} = \sqrt{(x_i - x_j)^2 + (y_i - y_j)^2 + (z_i - z_j)^2} = \sqrt{x_{ij}^2 + y_{ij}^2 + z_{ij}^2} \tag{A.3}$$

Equation (A.1) can be simplified for the purposes of calculation by using the following general vector identities

$$(\vec{a}\times\vec{b})\times\vec{c} = (\vec{a}\cdot\vec{c})\vec{b} - (\vec{b}\cdot\vec{c})\vec{a} \tag{A.4}$$

$$(\vec{a}\times\vec{b})\cdot(\vec{c}\times\vec{d}) = (\vec{a}\cdot\vec{c})(\vec{b}\cdot\vec{d}) - (\vec{a}\cdot\vec{d})(\vec{b}\cdot\vec{c}) \tag{A.5}$$

Using these and taking each term in (A.1) separately we can find that

$$(\vec{r}_{ij} \times \vec{\mu}_i) \times \vec{\mu}_j = (\vec{r}_{ij} \cdot \vec{\mu}_j)\vec{\mu}_i - (\vec{\mu}_i \cdot \vec{\mu}_j)\vec{r}_{ij} \tag{A.6}$$

$$(\vec{r}_{ij} \times \vec{\mu}_j) \times \vec{\mu}_i = (\vec{r}_{ij} \cdot \vec{\mu}_i)\vec{\mu}_j - (\vec{\mu}_i \cdot \vec{\mu}_j)\vec{r}_{ij} \tag{A.7}$$

$$\begin{aligned}(\vec{r}_{ij} \times \vec{\mu}_i) \cdot (\vec{r}_{ij} \times \vec{\mu}_j) &= (\vec{r}_{ij} \cdot \vec{r}_{ij})(\vec{\mu}_i \cdot \vec{\mu}_j) - (\vec{r}_{ij} \cdot \vec{\mu}_j)(\vec{\mu}_i \cdot \vec{r}_{ij}) \\ &= r_{ij}^2(\vec{\mu}_i \cdot \vec{\mu}_j) - (\vec{r}_{ij} \cdot \vec{\mu}_j)(\vec{\mu}_i \cdot \vec{r}_{ij})\end{aligned} \tag{A.8}$$

Then making the replacements (A.6)-(A.8) in (A.1) yields

$$\vec{F}_{mi} = \frac{3\mu_0}{4\pi r_{ij}^5}\left[(\vec{r}_{ij} \cdot \vec{\mu}_j)\vec{\mu}_i + (\vec{r}_{ij} \cdot \vec{\mu}_i)\vec{\mu}_j + (\vec{\mu}_i \cdot \vec{\mu}_j)\vec{r}_{ij} - \frac{5}{r_{ij}^2}(\vec{r}_{ij} \cdot \vec{\mu}_j)(\vec{\mu}_i \cdot \vec{r}_{ij})\vec{r}_{ij}\right] \tag{A.9}$$

This is a general result that we will expand and simplify under the assumptions (2.9a) and (2.9b) . Doing so gives

$$\vec{F}_{mi} = \frac{3\mu_0\mu_i\mu_j}{4\pi}\left(\frac{1}{r_{ij}^5}\begin{bmatrix} x_{ij} \\ y_{ij} \\ 3z_{ij}\end{bmatrix} - \frac{5}{r_{ij}^7}\begin{bmatrix} x_{ij}z_{ij}^2 \\ y_{ij}z_{ij}^2 \\ z_{ij}^3\end{bmatrix}\right) \tag{A.10}$$

In the above, if $i = j$ then it is a self force and we take $\vec{F}_{mi} = 0$. Also, it will necessarily be the case that $\vec{F}_{mi} = -\vec{F}_{mj}$.